ผลกระทบของการเหนี่ยวรั้งที่ปลายต่อสมรรถนะการทนไฟของแผ่นพื้นคอนกรีตแกนกลวง

นายชัยธร โฆษิตศรวณีย์

วิทยานิพนธ์นี้เป็นส่วนหนึ่งของการศึกษาตามหลักสูตรปริญญาวิศวกรรมศาสตรมหาบัณฑิต
สาขาวิชาวิศวกรรมโยธา ภาควิชาวิศวกรรมโยธา
คณะวิศวกรรมศาสตร์ จุฬาลงกรณ์มหาวิทยาลัย
ปีการศึกษา 2556
ลิขสิทธิ์ของจุฬาลงกรณ์มหาวิทยาลัย

บทคัดย่อและแฟ้มข้อมูลฉบับเต็มของวิทยานิพนธ์ปริญญาโทที่ส่งผ่านทางบัณฑิตวิทยาลัยเป็นแฟ้มข้อมูลที่ผู้ใช้งานสามารถค้นหาได้ผ่านทางคลังปัญญาจุฬาฯ (CUIR)
เป็นแฟ้มข้อมูลของนิสิตเจ้าของวิทยานิพนธ์ที่ส่งผ่านทางบัณฑิตวิทยาลัย
The abstract and full text of theses from the academic year 2011 in Chulalongkorn University Intellectual Repository(CUIR)
are the thesis authors' files submitted through the Graduate School.

EFFECT OF END RESTRAINT ON THE FIRE-RESISTANCE PERFORMANCE OF HOLLOW CORE CONCRETE SLABS

Mr. Chaiyatorn Kositsornwanee

A Thesis Submitted in Partial Fulfillment of the Requirements

for the Degree of Master of Engineering Program in Civil Engineering

Department of Civil Engineering

Faculty of Engineering

Chulalongkorn University

Academic Year 2013

Copyright of Chulalongkorn University

Thesis Title	EFFECT OF END RESTRAINT ON THE FIRE-RESISTANCE PERFORMANCE OF HOLLOW CORE CONCRETE SLABS
By	Mr. Chaiyatorn Kositsornwanee
Field of Study	Civil Engineering
Thesis Advisor	Associate Professor Thanyawat Pothisiri, Ph.D.

Accepted by the Faculty of Engineering, Chulalongkorn University in Partial Fulfillment of the Requirements for the Master's Degree

.....Dean of the Faculty of Engineering

(Professor Bundhit Eua-Arporn, Ph.D.)

THESIS COMMITTEE

.....Chairman

(Professor Thaksin Thepchatri, Ph.D.)

.....Thesis Advisor

(Associate Professor Thanyawat Pothisiri, Ph.D.)

.....Examiner

(Assistant Professor Withit Pansuk, Ph.D.)

.....External Examiner

(Assistant Professor Naret Limsamphancharoen, Ph.D.)

ชัยธร โฆษิตศรวณีย์ : ผลกระทบของการเหนี่ยวรั้งที่ปลายต่อสมรรถนะการทนไฟของแผ่นพื้นคอนกรีตแกนกลวง. (EFFECT OF END RESTRAINT ON THE FIRE-RESISTANCE PERFORMANCE OF HOLLOW CORE CONCRETE SLABS) อ.ที่ปรึกษาวิทยานิพนธ์หลัก : รศ.ดร.ธัญวัฒน์ โพธิศิริ, 75 หน้า.

ในการก่อสร้างอาคารได้มีการใช้งานแผ่นพื้นคอนกรีตแกนกลวงอย่างแพร่หลายเนื่องจากจุดเด่นของแผ่นพื้นคอนกรีตแกนกลวง ได้แก่ น้ำหนักเบา การติดตั้งสะดวกรวดเร็ว และการควบคุมคุณภาพแผ่นพื้นในกระบวนการผลิต อย่างไรก็ตาม ในภาวะเพลิงไหม้สมรรถภาพรองรับน้ำหนักบรรทุกของแผ่นพื้นคอนกรีตแกนกลวงมีแนวโน้มลดลงอย่างรวดเร็วภายใต้อุณหภูมิที่เพิ่มขึ้นและส่งผลให้เกิดการวิบัติของโครงสร้างได้ โดยที่อัตราการทนไฟของแผ่นพื้นขึ้นอยู่กับลักษณะการติดตั้งบริเวณฐานรองรับ ลักษณะการติดตั้งโดยทั่วไปของแผ่นพื้นคอนกรีตแกนกลวงคือการติดตั้งบนคานรองรับบริเวณปลายโดยการเสริมเหล็กเดือยเพื่อเพิ่มสมรรถนะรองรับโมเมนต์ลบที่จุดรองรับ และเททับหน้าด้วยคอนกรีตเสริมเหล็กป้องกันการแตกร้าวเนื่องจากอุณหภูมิ ลักษณะการติดตั้งดังกล่าวส่งผลให้เกิดการเหนี่ยวรั้งที่ปลายของแผ่นพื้นคอนกรีตแกนกลวงภายใต้อุณหภูมิสูง

การศึกษานี้มีวัตถุประสงค์เพื่อศึกษาผลกระทบของการเหนี่ยวรั้งที่ปลายต่อสมรรถนะการทนไฟของแผ่นพื้นคอนกรีตแกนกลวงด้วยการทดสอบตัวอย่างจำนวน 13 ชิ้นโดยใช้เพลิงไหม้มาตรฐาน ISO834 โดยพิจารณาผลกระทบของระยะเวลาให้ความร้อน ความหนาของแผ่นพื้น และอัตราส่วนน้ำหนักบรรทุกสำหรับตัวอย่างที่มีฐานรองรับแบบธรรมดา นอกจากนี้ยังพิจารณาพฤติกรรมของแผ่นพื้นคอนกรีตแกนกลวงที่ติดตั้งด้วยลักษณะแตกต่างกัน เพื่อศึกษาผลกระทบของการเหนี่ยวรั้งที่ปลาย จากผลการทดสอบพบว่าการเหนี่ยวรั้งตามแกน และการเหนี่ยวรั้งต่อการหมุนที่เกิดขึ้นภายใต้สภาวะอุณหภูมิสูงจากลักษณะการติดตั้งบริเวณปลายของแผ่นพื้นและคอนกรีตทับหน้า ส่งผลให้แผ่นพื้นมีสมรรถนะการทนไฟที่เพิ่มสูงขึ้นอย่างมีนัยสำคัญ

ภาควิชา วิศวกรรมโยธา ลายมือชื่อนิสิต .....

สาขาวิชา วิศวกรรมโยธา ลายมือชื่อ อ.ที่ปรึกษาวิทยานิพนธ์หลัก .....

ปีการศึกษา 2556 .....

5470167421 : MAJOR CIVIL ENGINEERING

KEYWORDS : HOLLOW CORE CONCRETE SLAB / FIRE-RESISTANCE PERFORMANCE / END RESTRAINT / FIRE TEST

CHAIYATORN KOSITSORNWANEE : EFFECT OF END RESTRAINT ON THE FIRE-RESISTANCE PERFORMANCE OF HOLLOW CORE CONCRETE SLABS

ADVISOR : ASSOC. PROF. THANYAWAT POTHISIRI, Ph.D., 75 pp.

Hollow core concrete slabs have been widely used in building construction due to key advantages in lighter weight, ease of installation and quality control of the fabrication process. However, the load-bearing capacity of hollow core concrete slabs tends to reduce dramatically in fire under elevated temperatures, leading to a structural collapse, depending on the installation details. A typical end detail for hollow core concrete slabs in practice is the slab-end beam connection in which the slab units are installed on cast-in-place supporting beams with embedded steel rebars to enhance the negative moment capacity at the support and an additional layer of concrete topping along with temperature steel. This installation induces the end restraint of hollow core concrete slabs at high temperature.

The current study aims to investigate the effect of end restraint on the behavior of hollow core concrete slabs through a series of fire tests. Thirteen specimens were tested using ISO834 standard fire curve. The effect of three factors including heating duration, slab thickness and load ratio were examined for simply supported specimens. The behavior of hollow core concrete slabs with varying end details were compared in order to examine the effect of end restraint. Based on the test results, the end restraint provided by the slab-end beam connection and concrete topping significantly enhanced the fire-resistance performance of hollow core concrete slabs due to the axial restraint and the rotational restraint at the support.

Department : Civil Engineering Student's Signature .....

Field of Study : Civil Engineering Advisor's Signature .....

Academic Year : 2013

ACKNOWLEDGEMENTS

The author wishes to express his deep appreciation and sincere gratitude to his thesis advisor, Associate Professor Thanyawat Pothisiri, Ph.D., for the guidance, assistance and constant support throughout his study at Chulalongkorn University. Grateful acknowledgements are due to Professor Thaksin Thepchatri, Ph.D., Assistant Professor Withit Pansuk, Ph.D., Assistant Professor Naret Limsamphanchareon, Ph.D. for their valuable comments and recommendations and Associate Professor Anil C. Wijeyewickrema for his guidance and support throughout the exchange program at Tokyo Institute of Technology.

The author is grateful to CPAC Co., Ltd. for providing the hollow core concrete slabs, Japan Student Services Organization (JASSO) and Graduate School of Chulalongkorn University for supporting the scholarship to participate in Young Scientist Exchange Program (YSEP) at Tokyo Institute of Technology.

Special Thanks are also extended to those who have helped directly and indirectly in the preparation of this thesis.

CONTENTS

Page

LIST OF TABLES

Page

LIST OF FIGURES

Page

CHAPTER I

INTRODUCTION

1.1 Background

Precast concrete slabs have been widely used in building construction. The precast slabs are generally fabricated by prestressing steel wires in a mold with end anchors, after which the concrete is placed and cured. The tension force in the steel wires is transferred as compression within the concrete slab units to enhance the flexural capacity. In order to reduce the overall weight of concrete, the slabs can be cast having hollow cores. These slabs are usually referred as hollow core concrete slabs.

The key advantage of hollow core concrete slabs to typical cast-in-place slabs is the ease of installation. Hollow core concrete slab units can be placed directly on the supporting beams with or without concrete topping and rebars. Moreover, because hollow core concrete slabs are typically pre-cast in a controlled environment, the quality of the products can be assured. Despite these advantages, data from previous studies [1-4] suggest that the hollow core concrete slabs may perform poorly under high-temperature conditions. Previous studies have reported several factors, i.e., concrete strength, water content, pre-compression force, concrete cover, aggregate type, load ratio and boundary condition, to affect the load-bearing performance of prestressed concrete slabs under fire [1-4]. The flexural collapse of prestressed concrete slabs has been indicated to be due to various factors, such as concrete spalling, transverse cracks and longitudinal cracks, leading to a premature rupture of the prestressing steel reinforcement [4].

It has been shown that the load-bearing behavior of hollow core concrete slabs exposed to fire may be affected by end restraint [5-10]. In typical construction where hollow core concrete slab units are placed continuously and the end gaps are filled

with concrete or mortar, the slab units cannot expand freely when they are heated due to axial restraint from nearby unheated slab units which acts as the thermal thrust at the heated slab section [5]. The position of the line of thrust affects the fire resistance of the restrained concrete slabs. The nearer the line of thrust to the soffit usually means the higher fire resistance [5]. Unlike most cast-in-place concrete floor systems, hollow core concrete slabs are generally installed as one-way slabs and the effect of thermal expansion is dominant in a single direction. As such, the details of end supports are important to the thermal restraint condition and the fire resistance of the hollow core concrete slabs.

One of the most frequently installed end details for hollow core concrete slabs in practice is the slab-end beam connection in which the slab units are installed on cast-in-place supporting beams with embedded dowel steel rebars and the gap between the ends of two adjacent slab units are filled with concrete. In some cases an additional layer of concrete topping is placed along with the temperature reinforcement. Figure 1.1 shows typical details of hollow core concrete slab installation. Note that the dowel steel bars are installed to enhance the negative moment capacity of the slab at the support.

The benefit of end restraint on the fire resistance of concrete slabs has been investigated by several studies [2-3,5-10]. It has also been reported that the restrained slab assembly is normally subject to lower deflection as well as reduced level of concrete spalling [8]. According to ACI 216-07 [11], prestressed concrete slabs having 20-mm concrete cover with restrained ends are allowed to be designated for a 4-hour fire resistance rating. Compared with the prestressed concrete slabs with unrestrained ends, a 55-mm concrete cover (carbonate aggregates) is required for a 4-hour fire resistance rating. Nevertheless, a few studies have also shown that the restrained condition, in some cases, fail to increase the fire resistance of prestressed concrete slabs [3, 9].

For hollow core concrete slabs, fire tests at the University of Ghent [10] showed that the restrained hollow core concrete slabs with sufficient axial restraint could perform well under fire, because the gap in the cracks was limited. The effect of axial restraint has also been investigated by Felinger [7] for limiting the vertical cracks, reducing the slip development and enhancing the shear capacity of hollow core

concrete slabs [7]. Because the benefit of axial restraints to enhancing the fire resistance of hollow core concrete slabs generally depends on the location of the thermal thrust [5], the installation details are deemed significant. To date, the effect of end restraint on the fire resistance due to typical details such as those shown in Fig. 1.1 has not been investigated, particularly for relatively thin hollow core slabs with thickness not exceeding 15 mm.

The current study aims to investigate the effect of end restraint on the fire performance of typically installed hollow core concrete slabs with slab-end beam connection and concrete topping. A series of fire tests on the hollow core concrete slabs with varying support conditions and concrete topping are conducted. Various data from the fire tests are collected, such as concrete spalling, vertical deflections and temperatures in order to examine the behavior of the slabs at elevated temperatures with and without the effect of end restraint.

1.2 Research Objectives

The current study aims to investigate the effect of end restraint on the fire resistance performance of typically installed hollow core concrete slabs with slab-end beam connection and concrete topping through a series of fire tests.

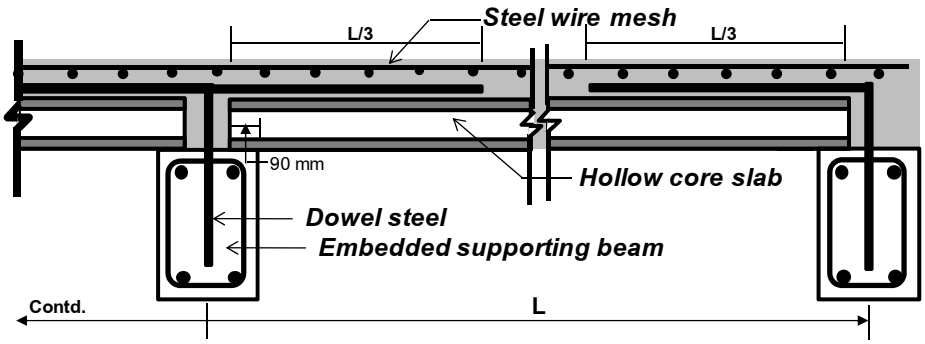

Figure. 1.1 Typical details of hollow core concrete slab installation

1.3 Scope of research

In order to examine the behavior of the hollow core concrete slabs at elevated temperatures and the effect of end restraint due to slab-end beam connection and concrete topping on the fire performance of hollow core concrete slabs, a series of fire tests were conducted for thirteen hollow core concrete slab specimens using ISO 834 standard fire curve [12]. Ten simply supported specimens without end restraint were tested to examine the effect of heating duration, slab thickness and load ratio, as summarized in Table 1.1. Three specimens were installed with slab-end beam connection and concrete topping with varying end details for the interior span and exterior span as summarized in Table 1.2. The test results are compared for the simply supported specimens and the test specimens with slab-end beam connection and concrete topping.

Table 1.1 Summary of simply supported test specimens

Specimen	*Width (mm)*	*Thickness (mm)*	*Length (mm)*	*Prestressing steel*	*Load ratio*	*Heating duration (min)*
TB1	600	120	2300	6 - Ø 4 mm	0.3	30
TB2	600	120	2300	6 - Ø 4 mm	0.3	60
TB3	600	120	2300	6 - Ø 4 mm	0.3	90
TB4	600	120	2300	6 - Ø 4 mm	0.3	120
LB1	600	100	2300	6 - Ø 4 mm	0.3	120
LB2	600	100	2300	6 - Ø 4 mm	0.6	120
LB3	600	120	2300	6 - Ø 4 mm	0.3	120
LB4	600	120	2300	6 - Ø 4 mm	0.6	120
LB5	600	150	2300	6 - Ø 4 mm	0.3	120
LB6	600	150	2300	6 - Ø 4 mm	0.6	120

Table 1.2 Summary of test specimens with end restraint

Specimen	*Width (mm)*	*Thickness (mm)*	*Length (mm)*	*Prestressing steel*	*Load ratio*	*Span location*	*Heating duration (min)*
SA01	600	100	2250	6 - Ø 4 mm	0.3	Exterior	210
SA02	600	120	2250	6 - Ø 4 mm	0.6	Exterior	210
SA03	600	150	2250	6 - Ø 4 mm	0.3	Interior	210

CHAPTER II

LITERATURE REVIEW

Concrete structures have widely been used in practice due to the superior strength and durability of concrete material at ambient condition. In addition, because of the material's low thermal conductivity, concrete structures have shown good performance at elevated temperatures [13]. Compared with steel, concrete allows a lower rate of temperature rise within the structures and hence an enhanced fire resistance rating. This chapter reviews data from the literature in order to examine the structural behavior of concrete slabs, particularly hollow core concrete slabs, exposed to heat as well as to identify the significance of the current research.

Several experimental studies [1,2,14,15] have been conducted to investigate the behavior of concrete slabs at elevated temperatures. These studies examine the effect of various parameters on the fire resistance and the failure mode of reinforced, prestressed and precast concrete slabs which can be summarized as follows.

Zheng *et al*. [1] have conducted an experimental study to examine the concrete spalling behavior of unbonded prestressed concrete slabs. Fifteen simply-supported slabs and nine two-span unbonded post-tensioned slabs were tested to investigate the influence of concrete strength, water content and stress levels at the pre-compression zone with respect to varying depths of specimens and numbers of prestressing steels. The fire tests were conducted in accordance with ISO 834 standard with no restraint against thermal expansion. The slabs were subjected to constant external loads during the tests, with varying load ratios between 0.32 and 0.59. Based on the test results, explosive concrete spalling was observed for eight simply-supported specimens and three two-span continuous specimens. All of the specimens with concrete spalling collapsed due to broken steel wires.

Bailey *et al*. [2] have examined the behavior of bonded post-tensioned concrete slabs at elevated temperatures. The test results of ten large-scale bonded post-

tensioned concrete slabs were reported with respect to varying duct materials, concrete aggregates and axial restraint conditions. The dimensions of the slabs were 4300 mm in length, 1600 mm in width and 160 mm in depth. During the fire test, each slab was loaded using four spread plates with a fixed load ratio of 0.6. During the 90-minute period of all fire tests, no collapse occurred. However, the slabs with siliceous aggregates were subject to much larger vertical deflections compared with the slabs with calcareous aggregates. Furthermore, the slabs with axial restraint were subject to lower deflections compared with the unrestrained ones.

Ali *et al*. [14] have conducted experimental and numerical studies on the behavior of reinforced concrete slabs exposed to standard fires with a focus on the occurrence of concrete spalling. Six full-scale normal strength concrete slabs were tested under ISO 834 and hydrocarbon fire curves. All of the six specimens had the same dimensions, 3300 mm in length, 1200 mm in width, 200 mm in depth and were subjected to a point load at mid-span with a load ratio of 0.65 during the test. The concrete mix and the material properties were controlled to be identical. The test results showed that all of the specimens could sustain 60-minute fire exposure but with different degrees of concrete spalling and mid-span deflection. It has been concluded that higher fire severity can lead the concrete slab to a higher degree of spalling and a higher rate of deflection.

Cooke [15] has investigated the behavior of precast concrete floors at elevated temperatures. Fourteen simply supported reinforced concrete slabs with 900-mm width and 4500-mm span were tested with varying slab thicknesses (150 mm and 250 mm), load levels (no load and 1.5 kN/m^2 live load), concrete types (normal-weight and light-weight concrete), soffit protection (no protection and gypsum board protection) and fire severity (ISO 834 and Norwegian Petroleum Directorate (NPD)). All of the slabs were designed to have a 90-minute fire resistance rating. During the fire tests, the temperature distribution within the slabs, the vertical deflection and the axial deformation were recorded. It was found that no collapse occurred after the 90-minute period. The vertical deflection was lower for slabs with a smaller thickness. Moreover, the light-weight concrete slabs deflected only two-thirds of the normal-weight concrete slabs, which was believed to be due to the lower thermal conductivity of light-weight concrete, leading the specimens to lower temperatures and lower

thermal expansion. Larger vertical deflections were also observed when the fire was more severe. The slabs subjected to the NPD fire deflected two times higher than the ISO 834 fire within the first 20 minutes of the fire test. The vertical deflections, however, could be reduced by using the gypsum board protection. No significant effect of load levels was observed because the mid-span deflections were induced dominantly by thermal bowing.

2.1 Flexural behavior of hollow core slabs at elevated temperatures

Concrete slabs are normally designed to carry mainly bending moments induced by imposed loads. As such, the load-bearing capacity of most concrete slabs is characterized by their flexural behavior. The flexural capacity of concrete slabs relies on the compressive strength of concrete and the tensile strength of steel rebars or prestressing tendons. At elevated temperatures, compression and tension zones on the cross sections of concrete slabs may shift due to temperature gradients. For hollow core concrete slabs, the temperature distribution may not be uniform through the thickness of the slabs due to the effect of air insulation inside the hollow cores [6]. Moreover, the mechanical properties of both concrete and steel can significantly deteriorate, leading to a reduced flexural capacity with respect to the increasing temperature.

The flexural failure mode of hollow core concrete slabs at normal temperature is characterized by transverse cracks propagated from the bottom surface due to bending moments from the imposed loads. These cracks can lead the prestressing wires to yield, after which the slabs can be subject to increasing deflections and larger cracks [7], and failure occurs once the prestressing wires are ruptured. However, at elevated temperatures the flexural failure of hollow core concrete slabs may occur rapidly due to a coupled effect between concrete spalling and longitudinal cracks. This combination can cause the prestressing wires to be exposed directly to fire, which can lead to premature wire rupture and failure of the hollow core concrete slabs [4].

2.2 Shear behavior of hollow core concrete slabs at elevated temperatures

The load-bearing capacity of hollow core concrete slabs is generally not governed by shear even though the shear resistance relies only on the web of the cross section. In general, shear failure of hollow core concrete slabs at normal temperature can be classified into two types [7]. The first type is called shear compression failure or flexural shear failure, which is caused by inclined shear cracks initiated by flexural cracks. This type of failure occurs in the areas with both bending moments and shear forces. The second type of failure is called shear tension failure, which normally occurs near the end of the support where the bending moment is relatively small.

Fellinger [7] has shown that the shear failure of hollow core concrete slabs at elevated temperatures is due to a combination of horizontal and vertical cracks through the web. Once this combined crack is large enough, the hollow core concrete slab would collapse due to shear failure. Unlike the flexural failure, the shear failure is brittle and hence more dangerous.

2.3 Concrete spalling

The fire resistance rating of typical concrete slabs can be governed by concrete spalling. Spalling of concrete cover can leave the prestressing steel subjected directly to heat, causing premature tendon rupture [4]. The occurrence of concrete spalling is related to the property of the cement paste [13]. When moisture within the cement paste is heated during the fire the vapour pressure is developed and the tensile stress is generated. Once this tensile stress exceeds the tensile strength of concrete, concrete spalling occurs. Previous studies [1,13] have reported various factors, such as moisture content, concrete strength, precompression force and fire severity, as crucial factors to the occurrence of concrete spalling.

2.4 Axial restraint

Axial restraint can provide a resisting effect to the thermal expansion of concrete structures at elevated temperatures. When a concrete member is heated, it tries to

expand and push against the unheated surrounding structures. As such, the thermal expansion is resisted by an axial thrust from the surrounding structures in each direction. This axial force is normally referred to as the thermal thrust, which acts like a prestressing force in the concrete structures [5, 16]. The location of the thermal thrust along the depth of the cross section is closely related to the fire resistance of the concrete structures [5]. For concrete floor systems, the axial restraint is provided based on the continuity of the slab system in each direction.

The axial restraint for hollow core concrete slabs is dominant in a single direction through “slab-end beam connection”. The actual construction details of the end connection may vary widely in practice. However, a typical detail includes the installation of steel rebars on the supporting beams. In addition, the gaps between the ends of adjacent slabs are filled with concrete and a layer of concrete topping is placed along with temperature steel reinforcement.

Figure 2.1 illustrates the structural behavior of a restrained simply supported slab [16]. When the slab is subjected to a distributed service load at normal temperature, the flexural moment is developed with the maximum positive moment (M^{+}_{max}) at mid-span. As long as the slab has no crack or damage, the nominal moment capacity (M^{+}_{n}) always exceeds the maximum positive moment as shown in Fig 2.1 (b). In case of fire, the concrete slab tends to lose its flexural strength at elevated temperatures due to the reduction in strength of steel and concrete. In addition, thermal cracks or other damages, e.g. concrete spalling and splitting cracks, may develop during the fire. As such, the nominal moment capacity is significantly reduced. If the concrete slab is unrestrained, it will collapse once the residual flexural strength at elevated temperature (M^{+}_{nt}) is less than the maximum positive moment. However, the situation is different for a restrained concrete slab in which the effect of thermal thrust provides additional moment capacity (M_T) as shown in Fig 2.1(c). During the fire, the thermal thrust acts at a distance d_t below the top surface. If the concrete slab is subjected to a mid-span deflection Δ, the additional moment capacity M_T at mid-span can be computed as $M_T = T(d_t - \Delta - a_t/2)$, in which a_t is the depth of the equivalent compressive stress block during the fire. This increase in the moment capacity enhances the fire resistance rating of the restrained concrete slab.

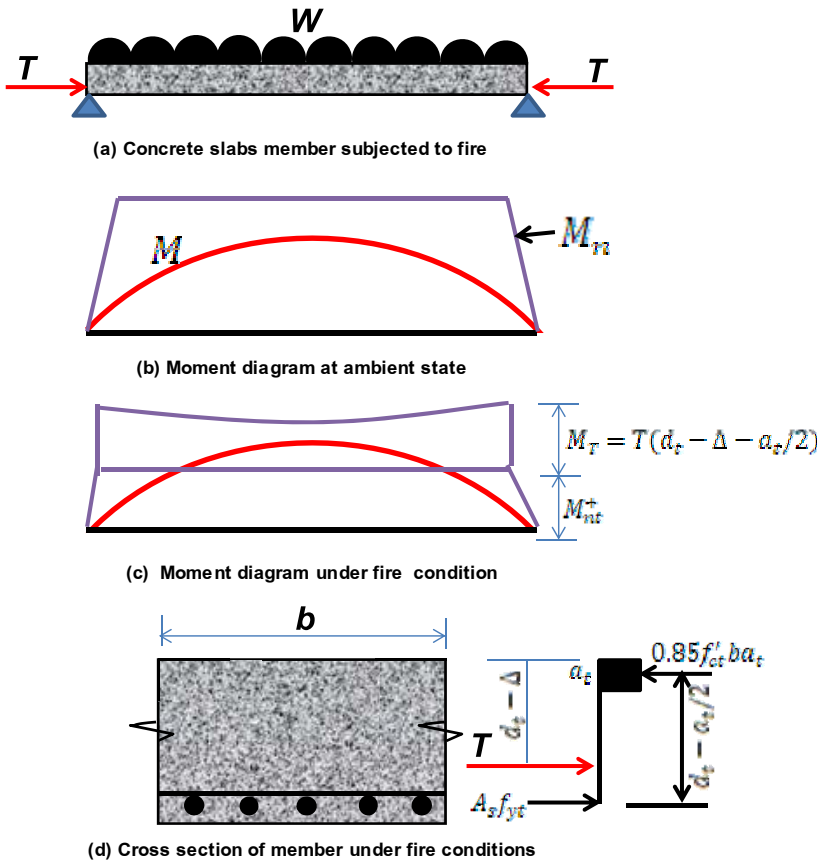

Figure 2.1 Moment diagrams for a restrained simply supported slab during fire [16]

A negative effect of the thermal thrust has also been reported in the literature [5]. When the thermal thrust is located below the neutral axis of the slab, the additional moment due to the thermal thrust will increase the moment capacity of the concrete slab. However, if the location of the thermal thrust lies above the neutral axis of the slab, the thermal thrust will induce an additional positive moment, causing the slab to fail earlier. The location of the thermal thrust generally depends on the details of the actual slab construction.

Bailey *et al*. [2] have investigated the effect of axial restraint on the fire performance of bonded post-tensioned concrete slabs. Ten one-way slab specimens were tested with a focus on the influence of duct materials, aggregate types and axial restraint conditions on the structural behavior of the concrete slabs at elevated temperatures. To investigate the effect of axial restraint conditions, two restraining steel beams were bolted to the loading frame to provide restraint against the horizontal expansion over the full depth of the specimens. It was shown that the specimens with

axial restraint had lower vertical deflections compared with the specimens without axial restraint. This effect could be observed for all types of aggregates and duct materials. However, the axial restraint did not significantly enhance the fire resistance rating of the specimens.

Fellinger *et al*. [7] have conducted a numerical study on the effect of axial restraint effect on shear and anchorage behavior of hollow core concrete slabs at elevated temperatures. Finite-element models were developed and validated using data from a series of fire tests. It was found that the restrained slabs are subject to smaller vertical cracks in the web and smaller prestressing wire slips compared with the unrestrained slabs. Furthermore, the restrained slabs had higher fire-resistance rating compared with unrestrained slabs. The fire resistance-rating was 159 min for the restrained slab with 200-mm depth and 123 min for the unrestrained slab with the same depth.

Another experimental study to investigate the effect of axial restraint on the behavior of hollow core concrete slabs was conducted by University of Ghent in Belgium [10]. Four tests of two floor spans were conducted under ISO 834 standard fire. The span of the specimens was 3 m long and the floor width was 2.4 m. At the middle of each span, the specimens were subjected to a 100-kN single line load. The dimensions of the specimens were varied, ranging between 200 mm and 265 mm in depth, 597 mm and 1196 mm in width. The objective of the tests was to investigate the effect of restrained condition, surrounding structures and concrete topping on the structural behavior of hollow core concrete slabs at elevated temperatures. The peripheral ties, which included the supporting edge beam at one end of the slab reinforced with two 12-mm diameter rebars and the longitudinal bars on both sides, were used to simulate the thermal restraint at the end and the surrounding structures. Based on the test results, only one specimen collapsed prior to 120 minutes due to concrete spalling. It was concluded that the failure time of the specimens was prolonged because the axial restraint could limit the occurrence of concrete cracks.

Moss *et al*. [5] have performed numerical analyses of the concrete slabs by using SAFIR finite element program. A 2D model of simply supported slabs with the depth of 200 mm, the width of 1000 mm and the span of 5000 mm was created. The slabs were subjected to ISO 834 standard fire curve with a maximum heating duration of 4

hours. The support condition, the position of the line of thrust and the level of axial restraint were examined. To provide different axial restraint conditions in the model, the spring element was used at the end of the slab. The stiffness of the spring element was relative to the axial stiffness of the specimens. Based on the analysis results, it was found that the position of the line of thrust was sensitive to the behavior of the concrete slabs under fire. The concrete slabs tended to have a higher fire resistance rating when the level of axial restraint was higher. The proposed value of spring stiffness in order to increase the flexural performance of the concrete slabs under fire was at least 50% of the axial stiffness. In addition, the line of thrust was beneficial to the concrete slabs when it is located at the bottom zone of the concrete slabs within 50 mm from the soffit. The vertical deflection of the concrete slabs was reduced if the line of thrust was located within this zone.

Wang [8] has examined the behavior of reinforced concrete slabs under various degrees of concrete spalling and axial restraint. A 3D model was developed using a non-linear finite element program called Vulcan. The study was based on a normal-weight reinforced concrete slab floor system with the dimensions of 37.5 x 37.5 m. The concrete floor system consisted of five 7.5 x 7.5 m concrete slab bays with a thickness of 250 mm. The slab was reinforced with two orthogonal steel rebars having 25-mm concrete cover at the soffit. Three types of supports were examined, i.e. simple support, completely fixed support and rotational fixed support without thermal restraint. The analysis results showed that the slab with a fixed support condition had an improved fire performance. Even in the most severe case of concrete spalling, in which the reinforcing steel bars were exposed directly to fire for 30 minutes, the concrete slab could reach more than 3-hour fire resistance. Compared with a simply-supported condition, the slabs collapsed within only 33 minutes. The vertical deflection at the middle of the slab was significantly affected by the support condition. The deflection of the slab with fixed ends was much lower than the simply supported slab. It was also observed that the thermal restraint was a major factor in reducing the impact of concrete spalling to the behavior of the reinforced concrete slab system due to the compressive membrane action developed by the thermal restraint.

Bailey *et al.* [3] have investigated the behavior of unbonded post-tensioned concrete slabs under fire using a non-linear finite element program called ABAQUS. The slabs were 4400 mm long, 1600 mm wide and 160 mm deep and were modeled only for one quarter due to symmetry. In order to study the effect of axial restraint on the unbonded post-tensioned slabs, the axial restraint was applied in the model relative to the axial stiffness of the slabs, ranging between ideally rigid and free to expand. The axial restraint position was also varied from 0.17 to 0.34 times the overall depth of the slabs from the soffit. Interestingly, the analysis results showed that when the slabs were subjected to the same position of axial restraint, the increasing axial restraint stiffness lowered the fire resistance rating, even though the vertical deflection at mid-span was reduced. The fire resistance rating of the ideally rigid restraint specimen was only 57 minutes, which was much lower than the free-to-expand slabs with up to 85-minute fire resistance.

Bailey *et al*. [9] have conducted a numerical study on the fire performance of bonded post-tensioned floor plates including the effect of axial restraint from shear wall. It was found that the fire resistance rating was not affected by the axial restraint.

Chang *et al*. [6] have investigated the effect of support conditions on the behavior of hollow core concrete slabs under fire. It was shown that the fire resistance rating was increased by the axial restraint due to the reduced vertical deflection.

2.5 Concrete topping

Concrete topping has been widely used as the top layer of the hollow core concrete slab system. The objectives of using concrete topping are to provide continuity between hollow core concrete units and to increase the load-bearing capacity of the hollow core concrete slab system. Girhammar *et al*. [17] have conducted experimental and analytical studies to investigate the shear performance of hollow core concrete slabs with concrete topping at normal temperature. Based on their results, concrete topping could improve the shear capacity of hollow core concrete slabs at normal temperature by 35%.

Previous studies on the effect of concrete topping on the behavior of the hollow core concrete slabs at elevated temperatures were still limited. However, based on

ASTM E119 [18] the use of concrete topping for hollow core concrete slabs can be classified as a restrained condition. This benefit of concrete topping in providing axial restraint should be confirmed through experimental investigations.

2.6 Rotational restraint

As mentioned previously, the continuity of precast concrete slabs can be provided through the insulation details at the supporting beam and concrete topping. The continuity of slabs improves the fire resistance due to the rotational restraint, which causes the slabs to be statically indeterminate. Because of higher redundancy against collapse, continuous slabs have better performance in fire than simply-supported slabs [6]. In fire situation, the simply-supported slabs collapse when a plastic hinge is formed at the mid span but the rotational restraint at both ends of the continuous slabs allows the load to be resisted through moment redistribution after the first plastic hinge occurs at the support [13]. The failure of continuous slabs will occur when the plastic hinges are formed at three positions as shown in Fig. 2.2.

The effect of rotational restraint can be combined with the effect of axial restraint during the fire to increase the fire resistance performance of slabs [6], depending on the installation details. The behavior of the hollow core concrete slabs with respect to different end details should be investigated through experimental investigations.

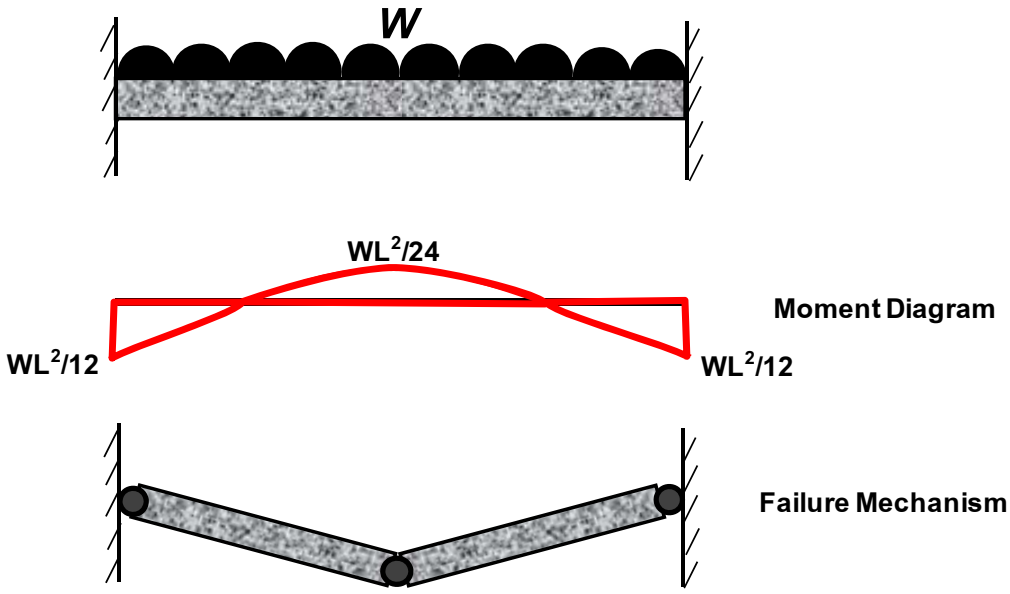

Figure 2.2 Behavior of a continuous slab with rotational restraint [13]

2.7 Research significance

Based on the literature review, it is seen that the fire performance of hollow core concrete slabs is affected by various factors, such as fire severity, type of aggregates, support condition and load level. Previous studies have shown the effect of rotational and axial restraints in improving the fire performance of hollow core concrete slabs. The beneficial effect of axial restraint depends upon the position of the line of thermal thrust which can vary based on the details of the slab construction. To gain the most benefit, the thermal thrust must be located below the neutral axis of the slab at a sufficient distance to counter-balance the effect of positive moments induced by external loading. For thin hollow core concrete slabs, the thermal restraint may fail to enhance the fire resistance.

The current research focuses upon the effect of end restraint due to the concrete end plugs and concrete topping on the fire performance of relatively thin hollow core concrete slabs. The specific details of concrete end plugs and concrete topping adopted for the current study are obtained from actual construction in practice.

CHAPTER III

EXPERIMENTAL INVESTIGATION OF HOLLOW CORE CONCRETE SLABS

In order to investigate the effect of end restraint on the fire resistance performance of hollow core concrete slabs, a series of fire tests were conducted. The behavior of simply supported hollow core concrete slabs under high-temperature conditions were examined with respect to three varying parameters: heat exposure time, thickness of slab and load ratio. The effect of end restraint due to concrete end plugs and concrete topping in accordance with the typical details in actual construction was examined for slabs in interior and exterior bays using different installation details. The test results are compared for hollow core concrete slabs with varying support conditions.

3.1 Test specimens

The test specimens were typical hollow core concrete slabs manufactured by CPAC Co., Ltd. under the company's quality control program. The summary of the test specimens are provided in Table 3.1. The dimensions of the simply supported specimens, TB01-TB04 and LB01-LB06, were 600 mm in width and 2300 mm in length while the dimensions of the remaining specimens, SA01-SA03, were 600 in width and 2250 mm in length in which the length was slightly reduced to accommodate the reinforcing steel at the supports. Note that the span length of the slab specimens was specified as governed by the dimensions of the furnace chamber. For the simply supported slabs, three values of thickness were examined, i.e. 100 mm, 120 mm and 150 mm, respectively. The nominal concrete strength of the specimens was specified as 35 MPa at 28 days. Each of the hollow core concrete slabs was reinforced with six 4 mm-diameter prestressing steel wires with a fixed concrete cover of 20 mm. The ultimate tensile strength of the prestrssing steel was 1850 MPa. The cross sections of the test specimens are illustrated in Fig. 3.1.

The specimens SA01-SA03, were installed with the concrete topping and different support conditions in order to simulate the typical details used in practice. Two concrete blocks representing supporting beams were installed at both ends. The dimensions of the concrete blocks were 200 mm in width, 300 mm in depth and 600 mm in length. In addition, two types of details were specified at the support for the exterior end and the interior end. For the interior end, a supplementary reinforced concrete block with a thickness of 700 mm measured from the outer edge of the supporting concrete block was cast to constitute a fixed plane of symmetry between the interior ends of two adjacent hollow core concrete slabs as illustrated in Fig. 3.2(a).The supplementary concrete block was reinforced with three 6-mm steel round bars. Two 9-mm steel round bars were installed as dowel bars at the support, with a length of 250 mm embedded in the supporting concrete block and a minimum length of 750 mm (1/3 span) embedded in the concrete topping over the hollow core concrete slab as illustrated in Fig. 3.2(a). For the exterior end, two 9-mm steel round bars were also installed as dowel bars as illustrated in Fig. 3.2(b) without an additional concrete block at the support. The test specimens designated as an exterior span were specified with the interior details at one end and the exterior details as at the other end while the test specimens designated as an interior span were specified with the interior details at both ends. For the specimens SA01-SA03, concrete topping was also installed with a constant thickness of 50 mm and a 250-mm x 250-mm wire mesh (4-mm diameter) for temperature reinforcement. During concrete casting, the fresh concrete was controlled not to fill the hollow core beyond a maximum length of 140 mm from the end of the slab using plastic cones.

Table 3.1 Summary of the test specimens

Specimen	*Width (mm)*	*Thickness (mm)*	*Length (mm)*	*Prestressing steel*	*Load ratio*	*Span location*	*Heating duration (min)*
TB01	600	120	2300	6 - Ø 4 mm	0.30	-	30
TB02	600	120	2300	6 - Ø 4 mm	0.30	-	60
TB03	600	120	2300	6 - Ø 4 mm	0.30	-	90
TB04	600	120	2300	6 - Ø 4 mm	0.30	-	120
LB01	600	100	2300	6 - Ø 4 mm	0.30	-	120
LB02	600	100	2300	6 - Ø 4 mm	0.60	-	120
LB03	600	120	2300	6 - Ø 4 mm	0.30	-	120
LB04	600	120	2300	6 - Ø 4 mm	0.60	-	120
LB05	600	150	2300	6 - Ø 4 mm	0.30	-	120
LB06	600	150	2300	6 - Ø 4 mm	0.60	-	120
SA01	600	100	2250	6 - Ø 4 mm	0.30	Exterior	210
SA02	600	100	2250	6 - Ø 4 mm	0.60	Exterior	210
SA03	600	100	2250	6 - Ø 4 mm	0.30	Interior	210

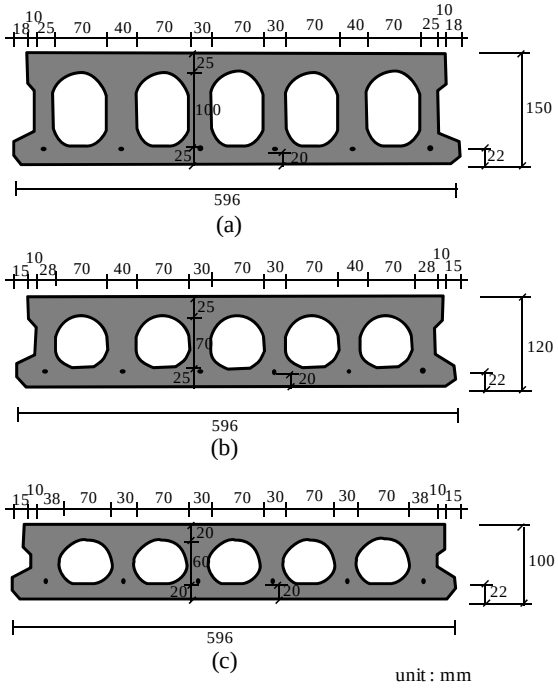

Figure 3.1 Cross sections of test specimens with different thicknesses: (a) 150 mm (b) 120 mm (c) 100 mm

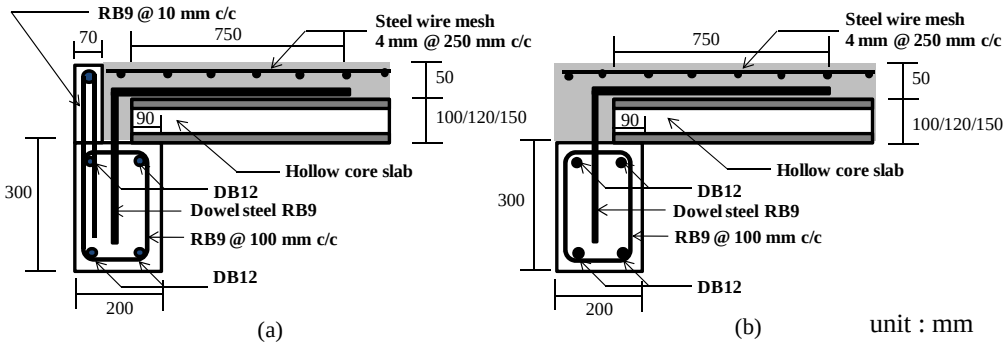

Figure 3.2 Details of end restraint: (a) interior end (b) exterior end

3.2 Test Set-up

The tests were carried out at the Fire Safety Research Center (FSRC), Chulalongkorn University. The details of the test setup can be described as follows.

3.2.1 Furnace

The dimensions of the initial furnace chamber were 2500 mm in length, 850 mm in width and 1800 mm in height prior to the installation of each hollow core concrete slab. During the course of the test, the soffit of the hollow core concrete slab was exposed to a specified heating condition inside the furnace chamber. The heating condition was controlled to follow the temperature-time relationship according to ISO 834 standard by using two sets of three LPG-fueled burners, which are located at the heights of 500 mm and 1150 mm, respectively, above the floor of the furnace. The temperatures inside the furnace chamber were monitored through six type-K thermocouples installed alongside the burners as illustrated in Fig. 3.3.

3.2.2 Specimen installation

The specimens TB01-TB04 and LB01-LB06 were installed inside the furnace chamber as simply supported one-way slabs on two steel-concrete composite blocks. The seating dimensions of each slab at both ends on the supports were specified as 200 mm to simulate the actual conditions of slab installation in practice. The details of the composite support are shown in Fig. 3.4. Note that one of the supports was

manufactured with a 200 mm x 500 mm opening to allow hot air exhaust outflow from the furnace chamber.

The specimens SA01-SA03 that were cast with supporting concrete blocks were installed directly onto the steel-concrete composite support at both ends.

To ensure the exposure to heat only at the soffit of the slab during the test, two insulating bars were installed on each side of the slab and ceramic fiber blankets were also used to cover the unexposed surface of the slab and the supporting concrete blocks as well as to fill any voids around the edges of the specimen.

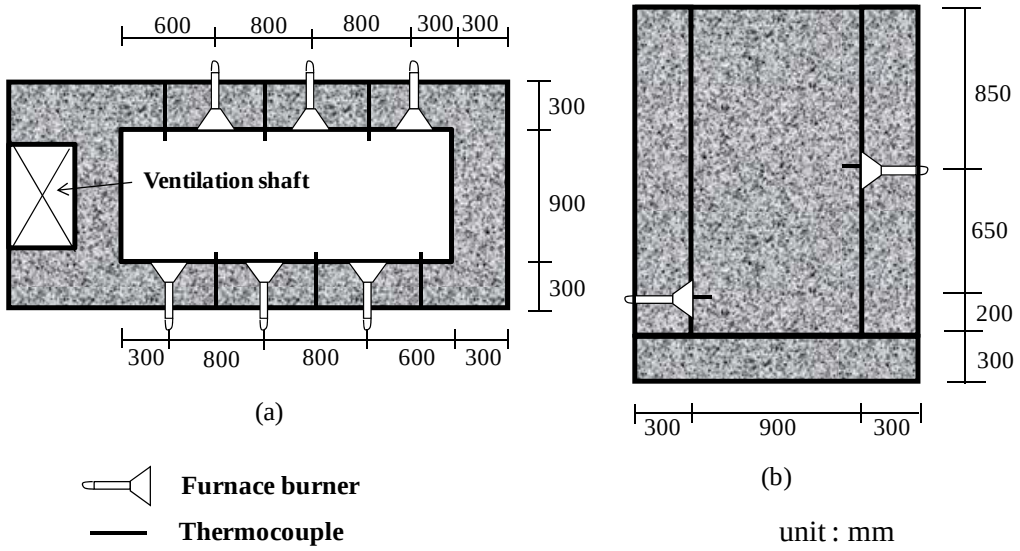

Figure 3.3 Furnace chamber: (a) horizontal section (b) vertical section

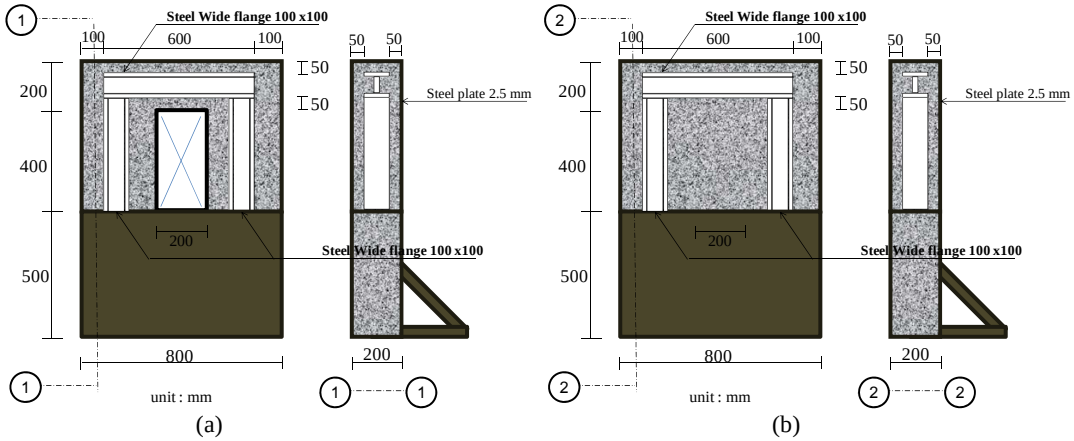

Figure 3.4 Supports for the specimen: (a) with ventilation opening
(b) without ventilation opening

3.2.3 Loading frame

During the course of the test, each specimen was subjected to a uniformly distributed load as determined by the specified load ratio. The load was initially applied as a point load by means of a hydraulic jack with 30-kN capacity. The applied load was transferred to the specimen using a mechanical device as shown in Fig. 3.5. Note that the contact points between the loading device and the slab specimen were allowed to rotate freely in the longitudinal direction to accommodate the vertical deflection of the slab during the test.

A load cell was installed between the hydraulic jack and the mechanical device to maintain a constant level of loading with respect to the specified load ratio. Fig. 3.6(a) and Fig. 3.6(b) illustrate the overview of the test set-up for the simply supported specimens and the specimen with end restraint.

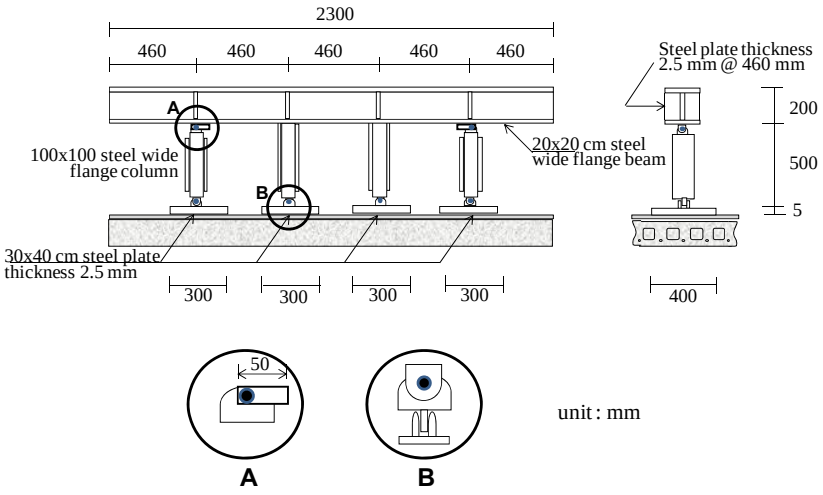

Figure 3.5 Details of the loading frame

3.3 Instrumentation

The temperatures of the hollow core concrete slabs were measured during the test using type-K thermocouple wires installed at fourteen different locations for the simply supported specimens and twenty-one locations for the test specimens with end restraint as shown in Fig. 3.7 The temperature data were recorded and collected through the Kyowa EDX-100A4H data acquisition system.

The vertical deflections of each hollow core concrete slab were also recorded during the test using three linear variable differential transducers (LVDT) with a measurement range of ±200 mm at mid-span and quarter-span as shown in Fig 3.7.

Post-fire investigations of the hollow core concrete slabs were conducted to quantify the severity of concrete spalling on the exposed side. A 50 mm x 50 mm grid system was used for mapping the locations and areas of concrete spalling. The depth of concrete spalling at each location was also recorded.

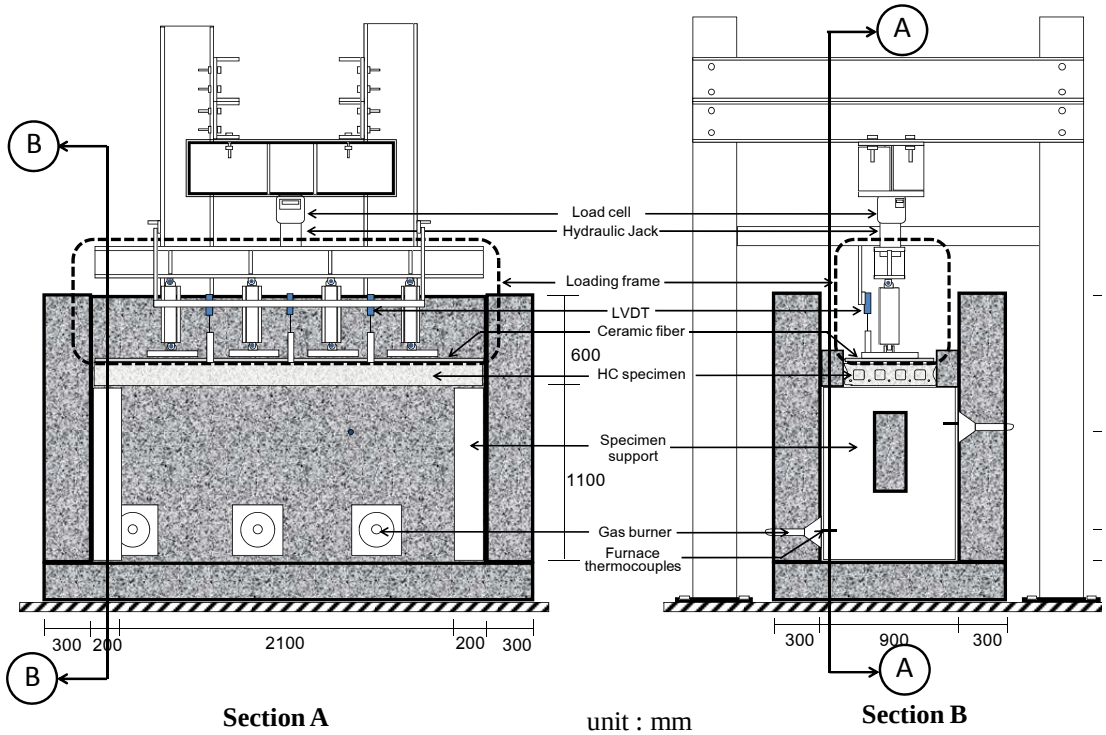

(a)

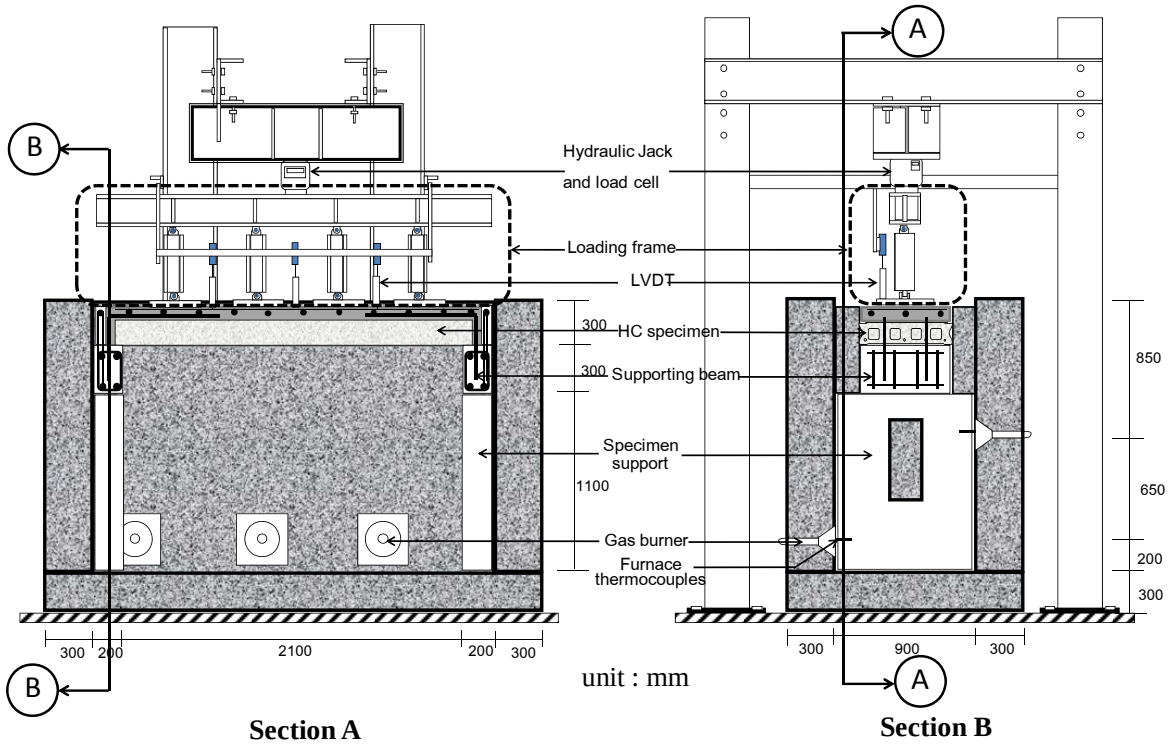

(b)

Figure 3.6 Test set-up: (a) simply supported specimens (TB01-TB06 and LB01-LB06) (b) specimens with end restraint (SA01-SA03)

(a)

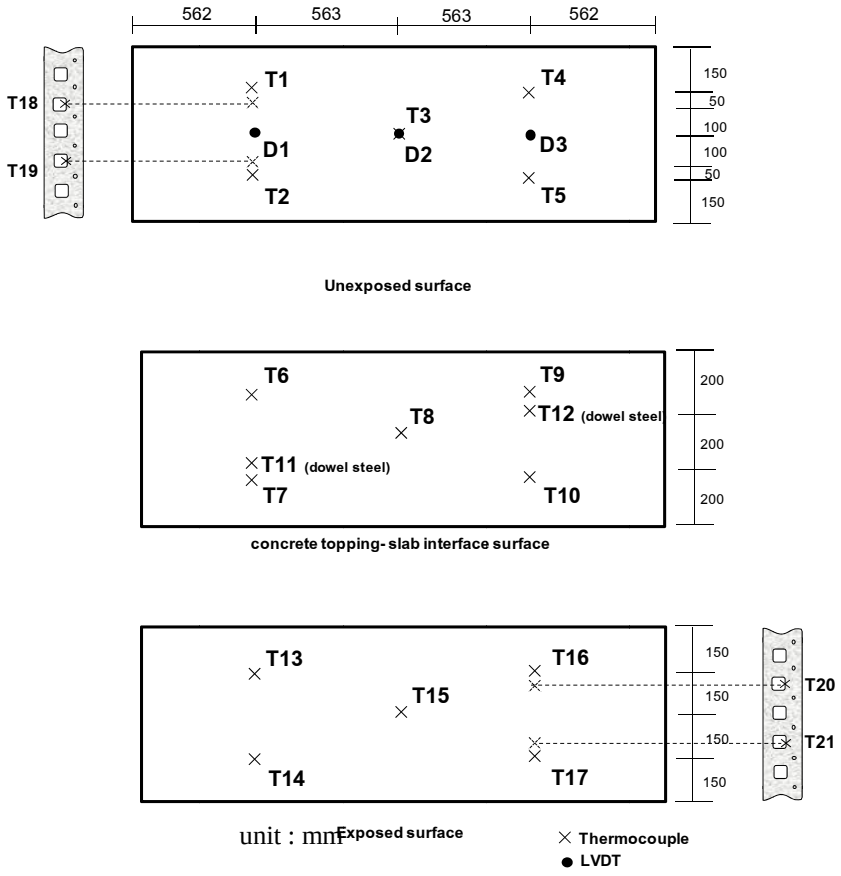

(b)

Figure 3.7 Locations of installed thermocouples: (a) simply supported specimens (TB01-TB06 and LB01-LB06) (b) specimens with end restraint (SA01-SA03)

3.4 Test Program

The test program was divided into three parts. The first part investigates the effect of heat exposure time on the fire-resistance performance of the hollow core concrete slabs. The second part investigates the effect of load ratio and thickness of slab on the fire-resistance performance of the hollow core concrete slabs. For the first and second test programs the effect of end restraint is not considered. The third test program investigates the effect of the end restraint on the fire-resistance performance of hollow core concrete slabs.

3.4.1 Termination criteria

As previously mentioned, the heating condition inside the furnace chamber was controlled to follow the temperature-time relationship according to ISO 834 standard. The heating duration was specified for each of the specimens. In addition, the following criteria for structural failure of ISO 834 were also used for the termination of the test [12].

a) Limiting deflection, $D = \frac{L^2}{400d}$ mm; and

b) Limiting rate of deflection, $\frac{dD}{dt} = \frac{L^2}{9000\,d}$ mm/min;

where L is the clear span of the test specimen (mm) and d is the distance from the extreme fibre of the design compression zone to the extreme fibre of the design tensile zone of the structural section (mm).

3.4.2 Load ratio

The applied load on each of the hollow core concrete slab specimens was calculated in terms of the ratio between the bending moment due to the applied load and the flexural capacity of the slab determined according to ACI 318-11 [20].

Two load ratios, 0.30 and 0.60, were adopted. Detailed calculations of the applied loads are shown in Appendix.

3.4.3 Test Program 1

To investigate the effect of the heating duration, four specimens with identical material properties and sectional dimensions, TB1-TB4, were tested. The load ratio was fixed at 0.30 for all of the specimens while the heating duration was varied at 30 min, 60 min, 90 min, and 120 min, respectively. Table 3.2 summarizes the specimen description for test program 1.

3.4.4 Test Program 2

In this test program, six hollow core concrete slab specimens with three varying thicknesses were tested under two different levels of load ratio. The material properties as well as the width and length of all the specimens were identical. The concrete cover of the prestressing steel for all the specimens was fixed at 20 mm. Table 3.3 summarizes the specimen description for test program 2.

3.4.5 Test Program 3

To investigate the effect of end restraint on the fire-resistance performance of hollow core concrete slabs, three specimens with two different support conditions were tested. The specimens SA01 and SA02 were designated as the exterior span and the specimen SA03 was designated as the interior span. Because of the likelihood of having a lower fire-resistance rating compared with the interior span, the exterior span specimens were subject to both levels of load ratio (0.3 and 0.6) while the interior span specimen was subject only to the load ratio of 0.6. The material properties as well as the width and the length of all specimens are identical. The maximum heating duration was set at 210 min. Table 3.4 summarizes the specimen description for specimens with end restraint.

Table 3.2 Specimen description for test program 1

Specimen	*Thickness of slab (mm)*	*Prestressing steel*	*Heating duration (min)*	*Load ratio*
TB01	120	6 -Ø 4 mm	30	0.30
TB02	120	6 -Ø 4 mm	60	0.30
TB03	120	6 -Ø 4 mm	90	0.30
TB04	120	6 -Ø 4 mm	120	0.30

Table 3.3 Specimen description for test program 2

Specimen	*Thickness of slab (mm)*	*Prestressing steel*	*Heating duration (min)*	*Load ratio*
LB01	100	6 -Ø 4 mm	120	0.30
LB02	100	6 -Ø 4 mm	120	0.60
LB03	120	6 -Ø 4 mm	120	0.30
LB04	120	6 -Ø 4 mm	120	0.60
LB05	150	6 -Ø 4 mm	120	0.30
LB06	150	6 -Ø 4 mm	120	0.60

Table 3.4 Specimen description for test program 3

Specimen	*Width (mm)*	*Thickness (mm)*	*Length (mm)*	*Prestressing steel*	*Load ratio*	*Span location*	*Heating duration (min)*
SA01	600	100	2250	6 - Ø 4 mm	0.3	Exterior	210
SA02	600	100	2250	6 - Ø 4 mm	0.6	Exterior	210
SA03	600	100	2250	6 - Ø 4 mm	0.6	Interior	210

3.5 Test Results

3.5.1 Test Program 1

The vertical deflections and concrete spalling of TB01 – TB04 are summarized in Table 3.5. Note that the TB04 test with a 120-min heating duration was canceled because the 120-mm thick slab was able to sustain only 82-minute heating duration based on TB03. The measured temperatures and vertical deflections during the tests can be shown in Fig. 3.8 and Fig. 3.9, respectively. The details of the test results are described below.

Table 3.5 Test results for test program 1

Specimen	*Heating duration (min)*	*Maximum vertical deflection (mm)*	*Concrete spalling*		
			Area (%)	*Maximum depth (mm)*	*Average depth (mm)*
TB01	*30*	*23.7*	*0*	-	-
TB02	*60*	*31.4*	*77*	*3*	*2*
TB03	*82*	*57.5*	*100*	*10*	*5*
TB04	*Canceled due to failure of TB03*				

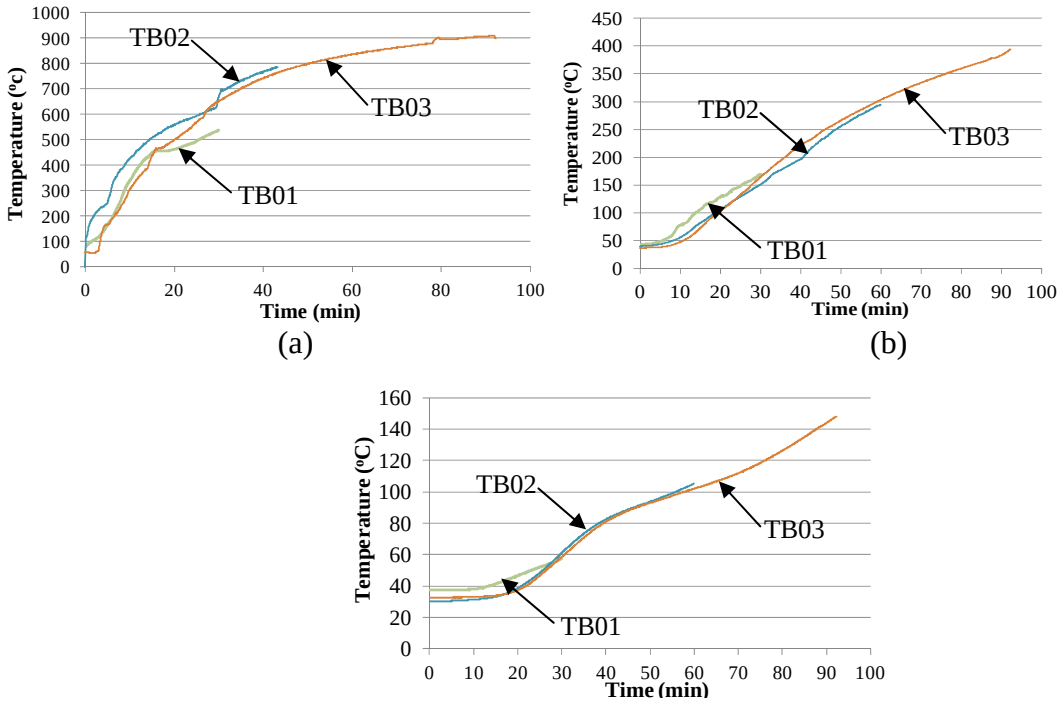

Figure 3.8 Temperature vs. time for TB01 – TB03: (a) exposed surface (b) hollow core (c) unexposed surface

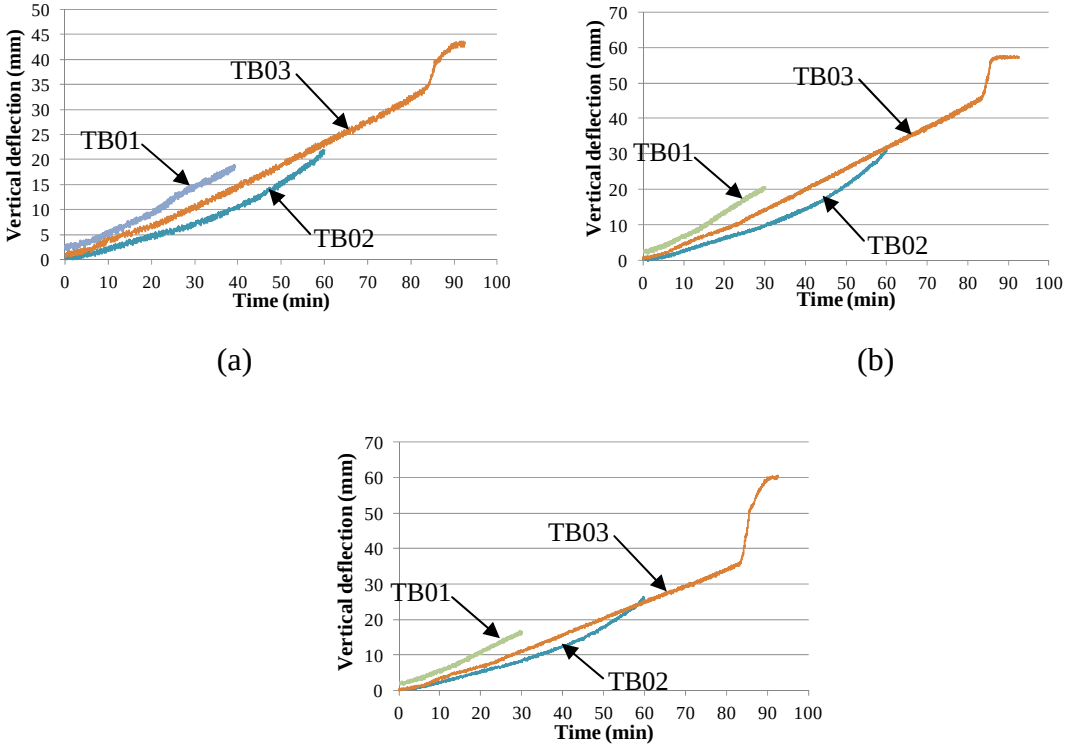

Figure 3.9 Vertical deflection vs. time for TB01 – TB03: (a) 1st quarter (b) mid-span (c) 3rd quarter

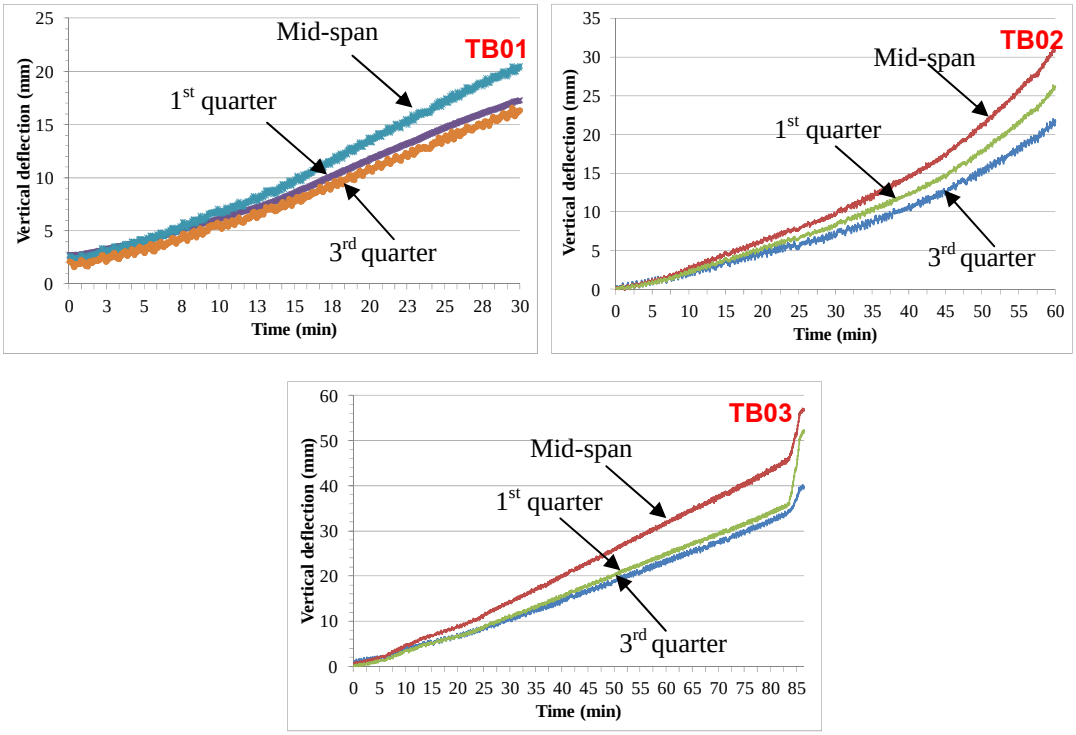

Figure 3.10 Vertical deflection vs. time for TB01 – TB03

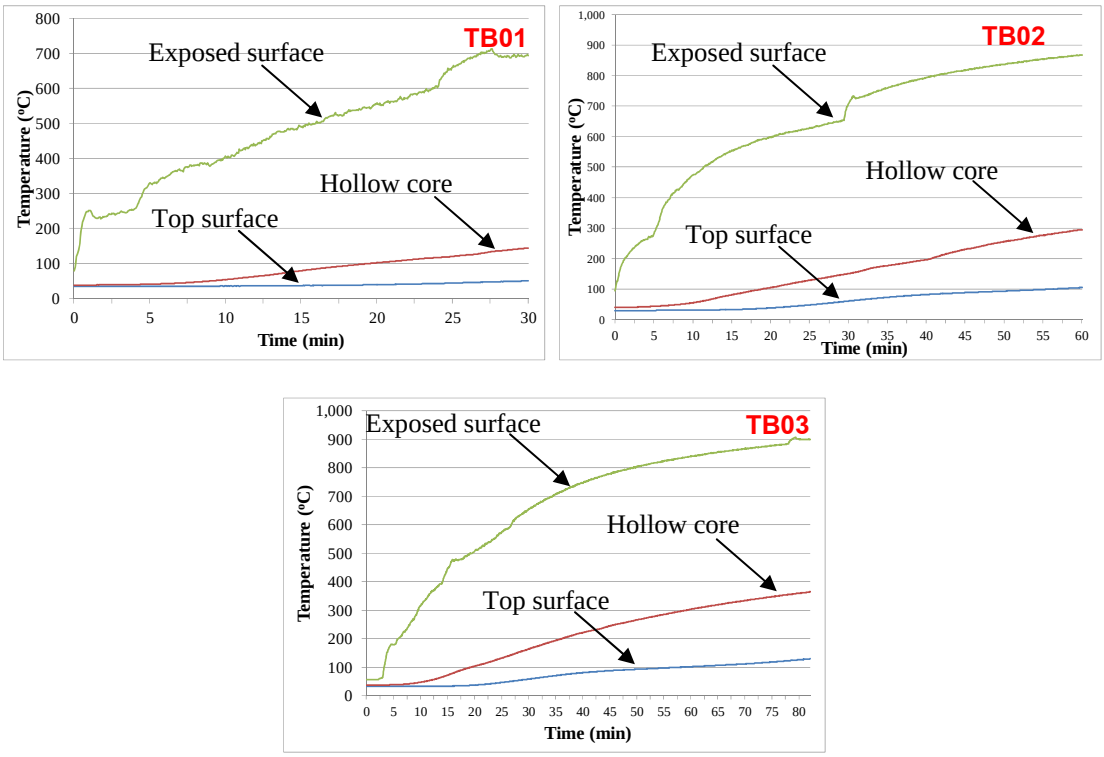

Figure 3.11 Temperature vs. time for TB01 – TB03

3.5.1.1 TB01

TB01 was subjected to the applied load with a load ratio of 0.3. During the 30-min heating duration, the average temperature of the exposed surface reached 712^{o}C. The temperature gradients between the exposed and unexposed surfaces and between the exposed surface and hollow core after 30 minutes were 662^{o}C and 568^{o}C, respectively, as shown in Fig. 3.11. The maximum vertical deflection of the specimen was 23.7 mm at mid-span after the 30-min heat exposure. The slab remained intact without collapse. No concrete spalling was observed on the exposed surface of the specimen as shown in Fig 3.12.

3.5.1.2 TB02

TB02 was also subjected to the applied load at the same load ratio of 0.3 as TB01 but was heated for 60 minutes. After the 60-min heating duration, the maximum vertical deflection recorded at mid-span was 31.4 mm while the average temperature of the exposed surface was 867^{o}C. The temperature gradients between the exposed and unexposed surfaces and between the exposed surface and hollow core after 60 minutes were 762^{o}C and 573^{o}C, respectively, as shown in Fig. 3.11. The post-fire investigation of TB02 revealed that 77% of the exposed surface area was subject to concrete spalling with an average depth of 2 mm. In addition, a transverse crack was observed near mid-span as shown in Fig 3.13. However, the specimen did not fail during the test.

3.5.1.3 TB03

TB03 was also subjected to the applied load with the same load ratio as TB01 and TB02, and the heating duration was specified at 90 minutes. However, the specimen collapsed after 82 minutes of heat exposure based on the rate of the deflection criterion of ISO 834. As can be seen in Fig. 3.9 and Fig. 3.10, the maximum deflection recorded was 57.5 mm at mid-span and the average temperature of the exposed surface reached 907^{o}C after the 82-min heating duration. The temperature gradients between the exposed and unexposed surfaces and between the exposed surface and hollow core after the 82 minutes were 759^{o}C and 514^{o}C, respectively. The

post-fire investigation revealed a transverse crack on the exposed surface near the support as shown in Fig. 3.14. For TB03, the entire exposed surface area was subject to concrete spalling with an average depth of 10 mm.

Fig 3.12 TB01 after fire test

Figure 3.13 TB02 after fire test

Figure 3.14 TB03 after fire test

3.5.2 Test Program 2

As previously mentioned, six specimens were tested to examine the effect of thickness of slab and load ratio on the fire-resistance performance of hollow core concrete slabs. The heating duration was specified at 120 minutes for all of the specimens. However, based on the test results all of the specimens collapsed prior to the specified heating period as shown in Table 3.6. The temperatures and vertical deflections recorded during the fire tests are illustrated in Fig. 3.15 and Fig. 3.18, respectively. The details of the test results are described below.

Table 3.6 Test results for test program 2

Specimen	***Heating duration (min)***	***Maximum vertical deflection (mm)***	***Concrete spalling***		
			Area (%)	***Maximum depth (mm)***	***Average depth (mm)***
LB01	*107*	*140.3*	*100*	*15.0*	*10.0*
LB02	*53*	*91.0*	*84*	*5.0*	*3.0*
LB03	*91*	*58.1*	*100*	*10.0*	*7.5*
LB04	*33*	*38.8*	*0*	-	-
LB05	*66*	*51.2*	*85*	*7.5*	*2.5*
LB06	*39*	*no measurements taken due to brittle failure*			

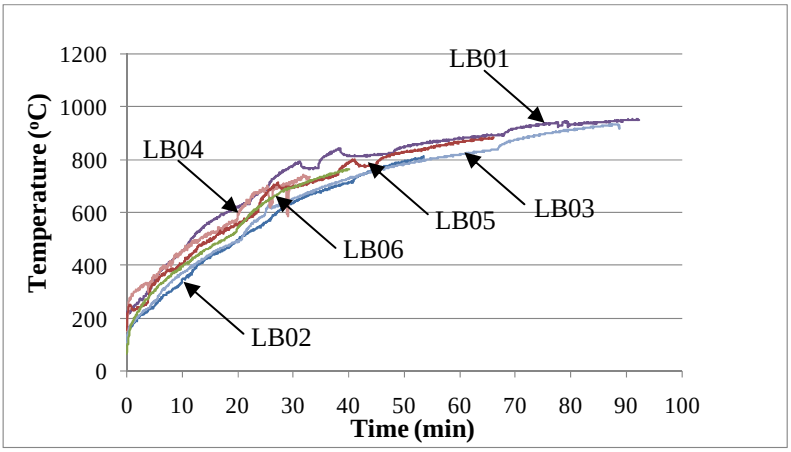

(a)

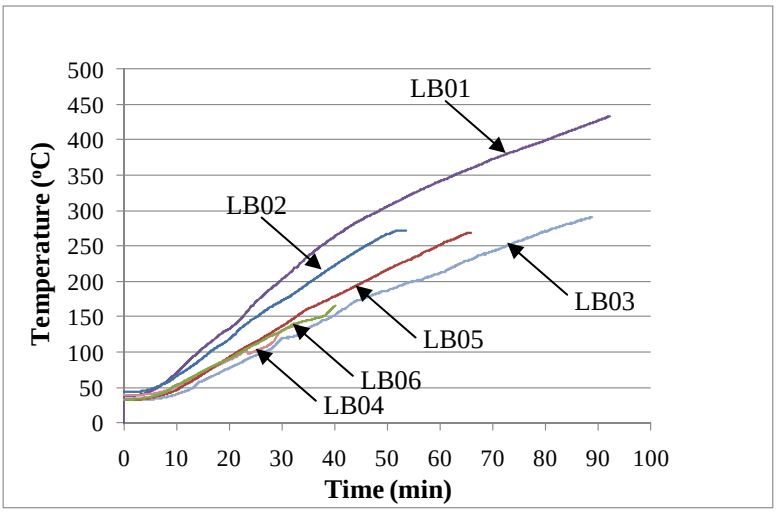

(b)

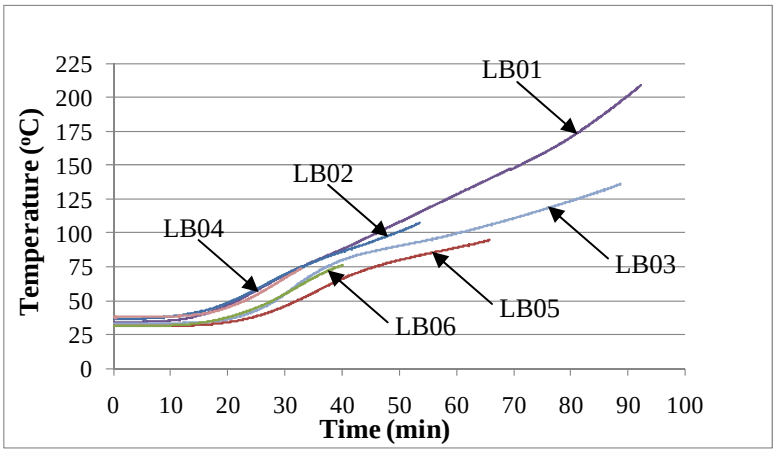

(c)

Figure 3.15 Temperature vs. time for LB01 – LB06: (a) exposed surface (b) hollow core (c) unexposed surface

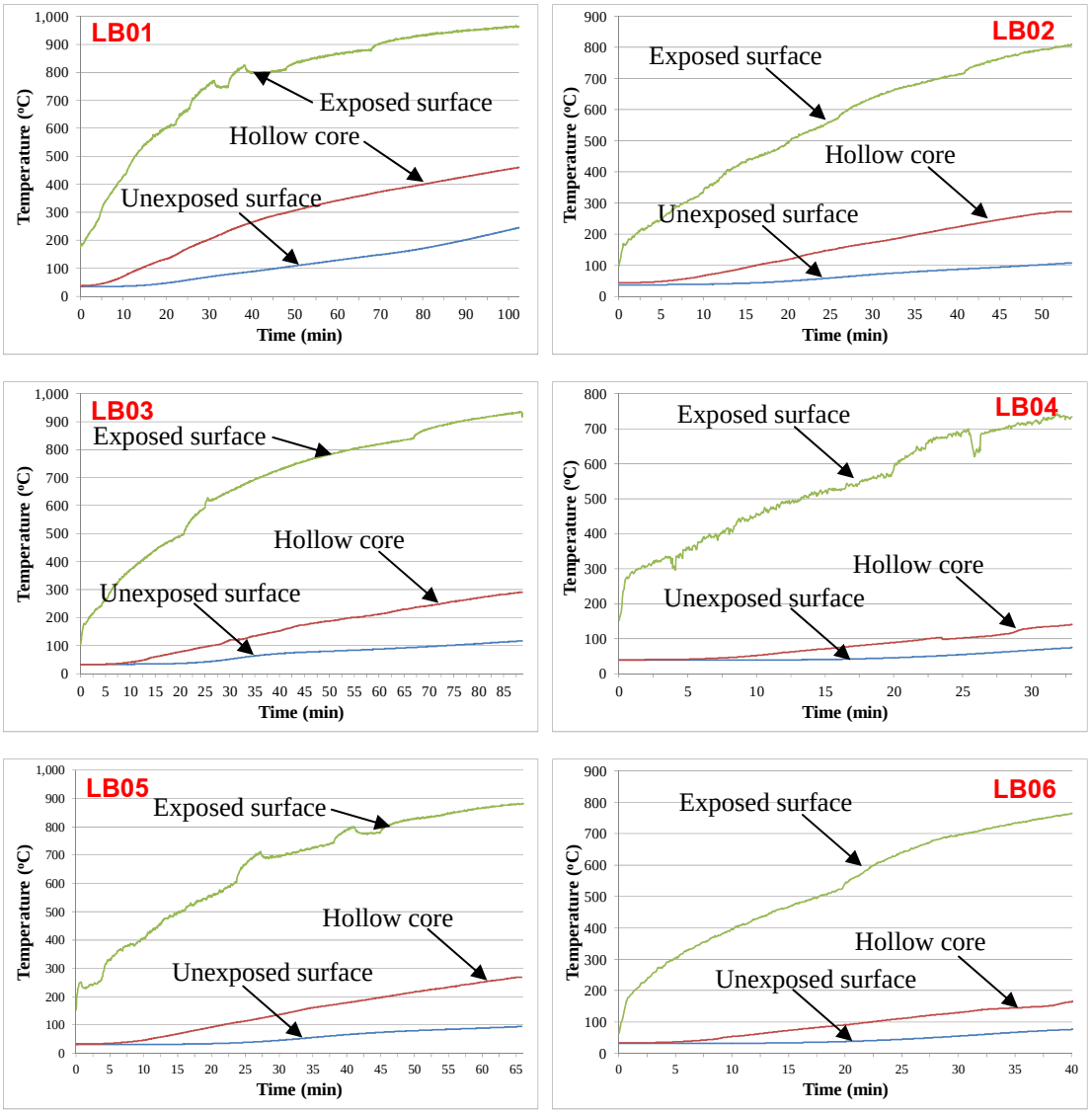

Figure 3.16 Temperature vs. time for LB01 – LB06

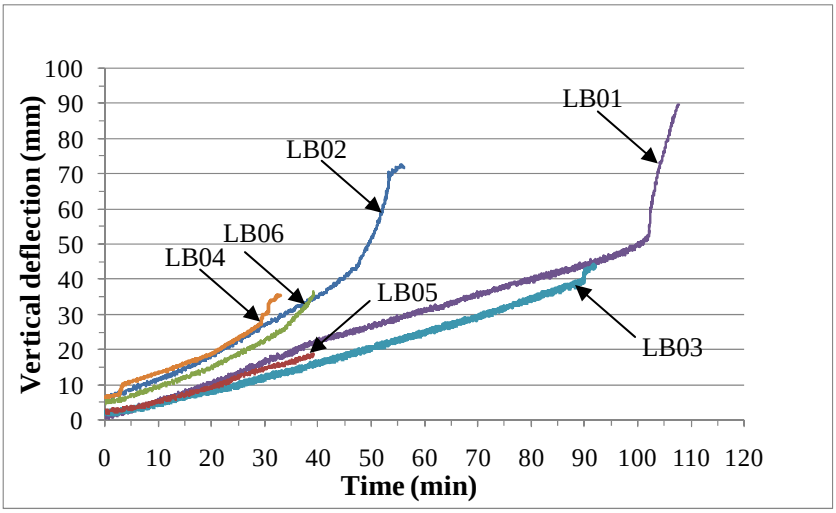

(a)

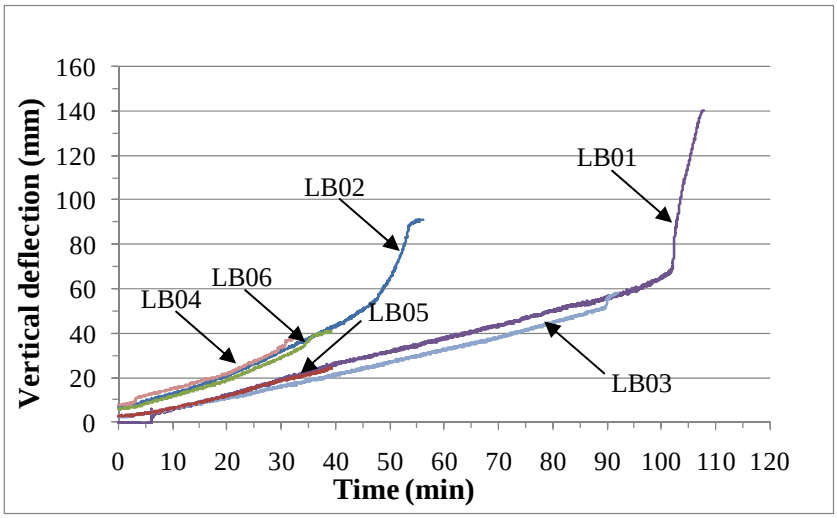

(b)

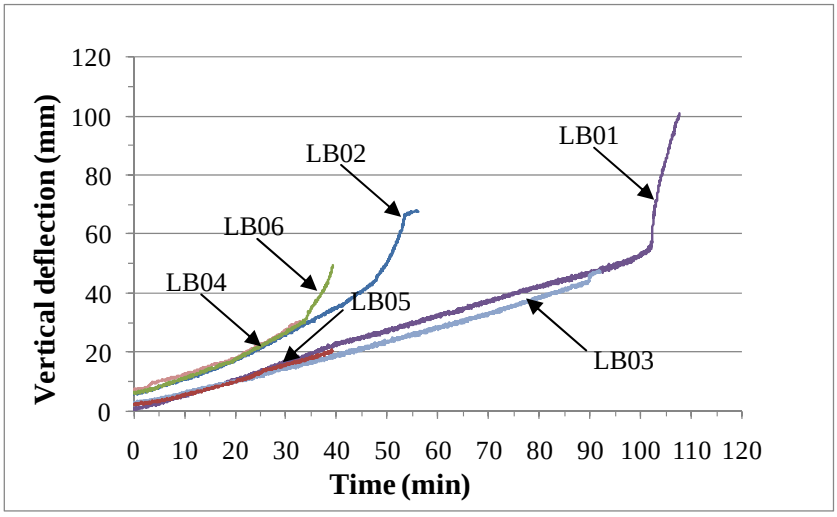

(c)

Figure 3.17 Vertical deflection vs. time for LB01 – LB06: (a) 1st quarter (b) mid-span (c) 3rd quarter

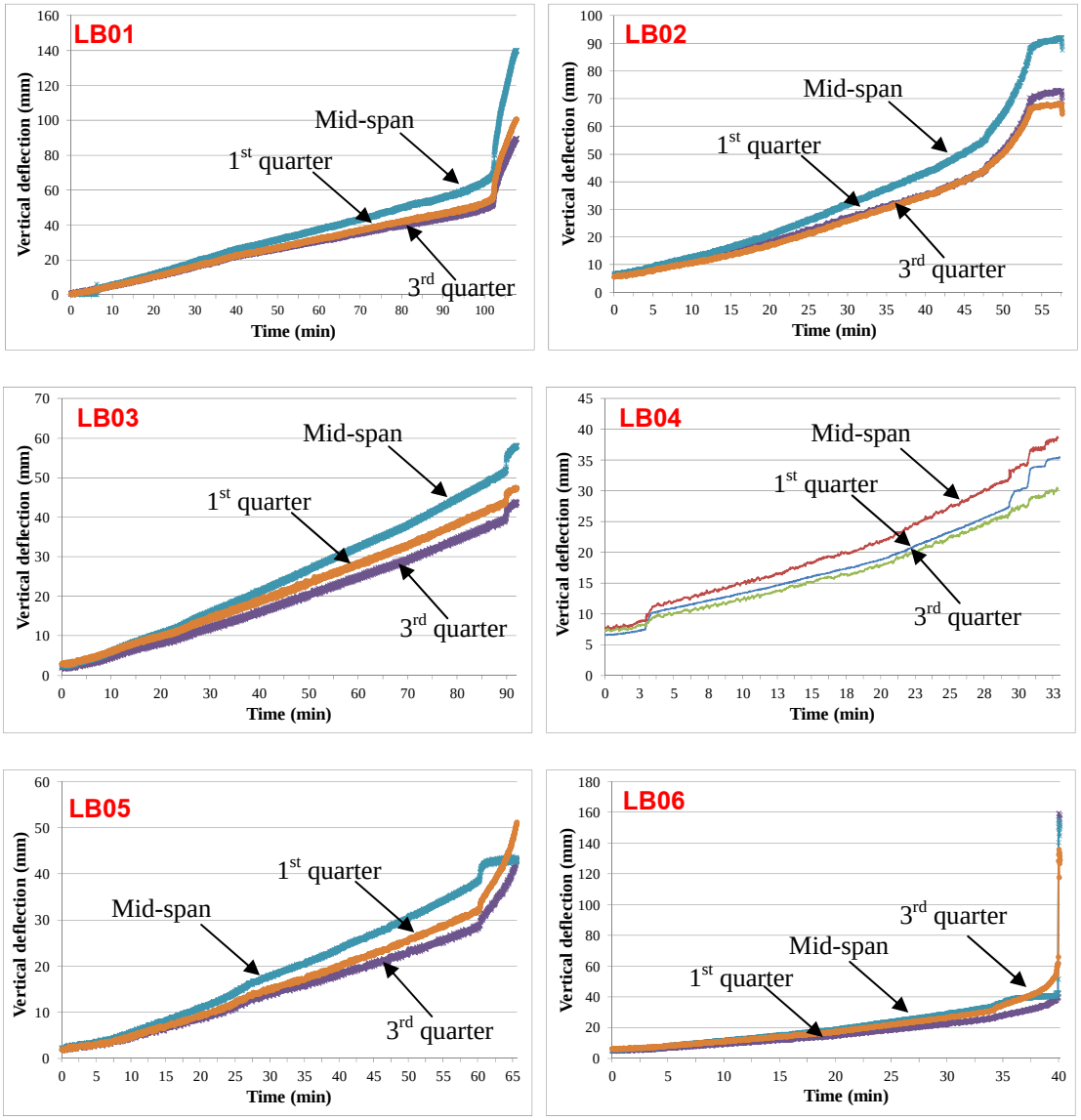

Figure 3.18 Vertical deflection vs. time for LB01 – LB06

3.5.2.1 LB01

LB01 was tested until failure under the applied load with a specified load ratio of 0.3. Based on the test results, the specimen failed due to the rate of deflection criterion after 107 minutes of heat exposure. The maximum vertical deflection recorded at mid-span was 140.3 mm and the average temperature of the exposed surface was 963^{o}C at failure. The temperature gradients between the exposed and unexposed surfaces and between the exposed surface and hollow core after 107 minutes were 719^{o}C and

503^{o}C, respectively. From the post-fire examination, it was found that concrete spalling occurred over the entire exposed area with an average depth of 10 mm and a maximum depth of 15 mm. A large transverse crack was also observed near mid-span as shown in Fig. 3.19.

3.5.2.2 LB02

LB02 had the same thickness of 100 mm as LB01 but was subjected to a higher load ratio of 0.6. The test was terminated after 53 minutes of ISO 834 standard fire exposure based on the rate of deflection criterion with a maximum vertical deflection recorded at mid-span of 91 mm, which was smaller compared with LB01. The average temperature of the exposed surface reached 812^{o}C at failure. The temperature gradients between the exposed and unexposed surfaces and between the exposed surface and hollow core after the 53-min heating period were 704^{o}C and 539^{o}C, respectively. Despite a higher load ratio compared with LB01, concrete spalling was observed on only 84% of the exposed area with an average depth of 3 mm and a maximum depth of 5 mm. In terms of concrete spalling, the severity of damage was much lower compared with LB01. Nonetheless, the post-fire investigation revealed a transverse crack near mid-span on the exposed surface as shown in Fig. 3.20.

3.5.2.3 LB03

The thickness of LB03 was 120 mm and the load ratio was specified as 0.3. The test results can be used to cross-check with TB03. It was found from the test that LB03 failed after 91 minutes of fire exposure based on the rate of deflection criterion of ISO 834 standard. The fire-resistance rating of LB03 is a bit higher compared with TB03 at 82 minutes. The average temperature of the exposed surface reached 930^{o}C at failure. The temperature gradients between the exposed and unexposed surfaces and between the exposed surface and hollow core after the 91-min heating period were 813^{o}C and 640^{o}C, respectively. The maximum vertical deflection recorded at mid-span at failure was 58.1 mm. Even though the entire exposed area of the specimen was subject to concrete spalling with an average depth of 7.5 mm and a maximum

depth of 10 mm, no evidence of transverse crack was observed as can be seen in Fig 3.21.

3.5.2.4 LB04

The thickness of LB04 was the same as LB03 but the load ratio was higher at 0.6. The fire test was terminated after 33 minutes of heat exposure based on the rate of deflection criterion. After the 33-min heating period, the maximum vertical deflection recorded at mid-span was 38.8 mm and the average temperature of the exposed surface was 744^{o}C. The temperature gradients between the exposed and unexposed surfaces and between the exposed surface and hollow core after the 33-min heating period were 673^{o}C and 608^{o}C, respectively. Interestingly, virtually no concrete spalling was observed on the exposed surface of the specimen. However, a severe transverse crack was observed near the support as shown in Fig. 3.22. Note that the longitudinal crack at the support was an extraneous damage as a result of hoisting the specimen which occurred after the fire test.

3.5.2.5 LB05

The thickness of LB05 was 150 mm, which was the largest among all of the test specimens, while the load ratio was specified as 0.3. Based on the test results, the specimen failed after 66 minutes of standard fire exposure based on the rate of deflection criterion. The maximum vertical deflection recorded after the 66-min heating duration was 51.2 mm, which occurred at the first quarter. The average temperature of the exposed surface of the specimen was 882^{o}C at failure. The temperature gradients between the exposed and unexposed surfaces and between the exposed surface and hollow core after the 66-min heating period were 788^{o}C and 614^{o}C, respectively. Based on the post-fire examination, a transverse crack was observed near mid-span on the exposed surface while the longitudinal crack was an extraneous damage as a result of hoisting the specimen which occurred after the fire test. Concrete spalling was observed over 85% of the exposed surface area with an average depth of 2.5 mm and a maximum depth of 7.5 mm. Fig 3.23 illustrates LB05 after the fire test.

3.5.2.6 LB06

LB06 had the same thickness as LB05 but was subjected to a higher load ratio at 0.6. Surprisingly, the specimen abruptly collapsed after 39 minutes of heat exposure without any significant warning. Fig 3.24 illustrates the remaining LB06 after collapse. No significant measurements could be taken due to brittle failure. The average temperature of the exposed surface prior to failure was 764^{o}C while the maximum vertical deflection recorded at mid-span was 40.7 mm. The temperature gradients between the exposed and unexposed surfaces and between the exposed surface and hollow core prior to failure were 688^{o}C and 600^{o}C, respectively. In addition, the post-fire investigation of damage revealed tendon rupture as well as transverse and longitudinal cracks on the exposed surface. The longitudinal cracks were also observed along the web of the hollow cores.

Figure 3.19 LB01 after fire test

Figure 3.20 LB02 after fire test

Figure 3.21 LB03 after fire test

Figure 3.22 LB04 after fire test

Figure 3.23 LB05 after fire test

(a) (b)

Figure 3.24 LB06 after fire test

3.5.3 Test Program 3

The test results of SA01-SA03 are summarized in Table 3.7. The temperatures and vertical deflections measured during the fire test are shown in Fig.3.25-Fig.3.28.

Table 3.7 Test results for test program 3

Specimen	*Load ratio*	*Span location*	*Test duration (min)*	*Maximum deflection (mm)*
SA01	0.3	Exterior	210	39.0
SA02	0.6	Exterior	210	49.3
SA03	0.6	Interior	210	46.4

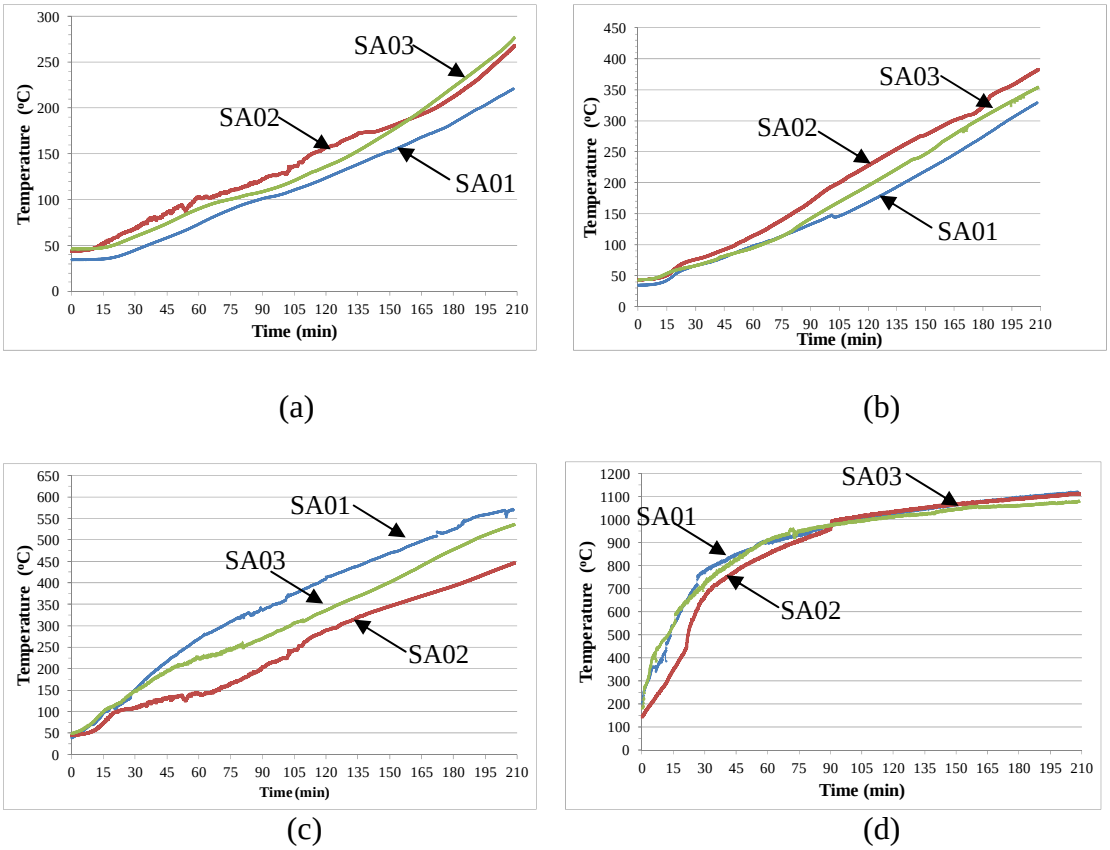

Figure 3.25 Temperature vs. time for SA01 - SA03: (a) unexposed surface (b) concrete topping - slab interface (c) hollow core (d) exposed surface

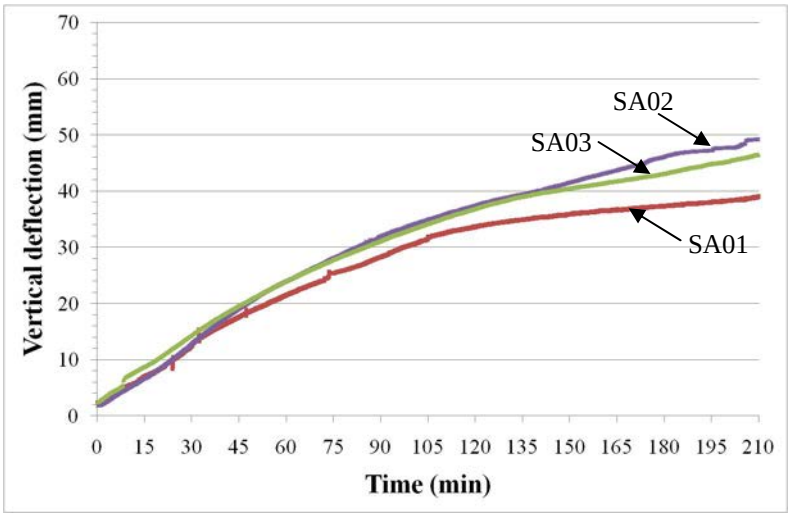

Figure 3.26 Maximum vertical deflection vs. time for SA01 -SA03

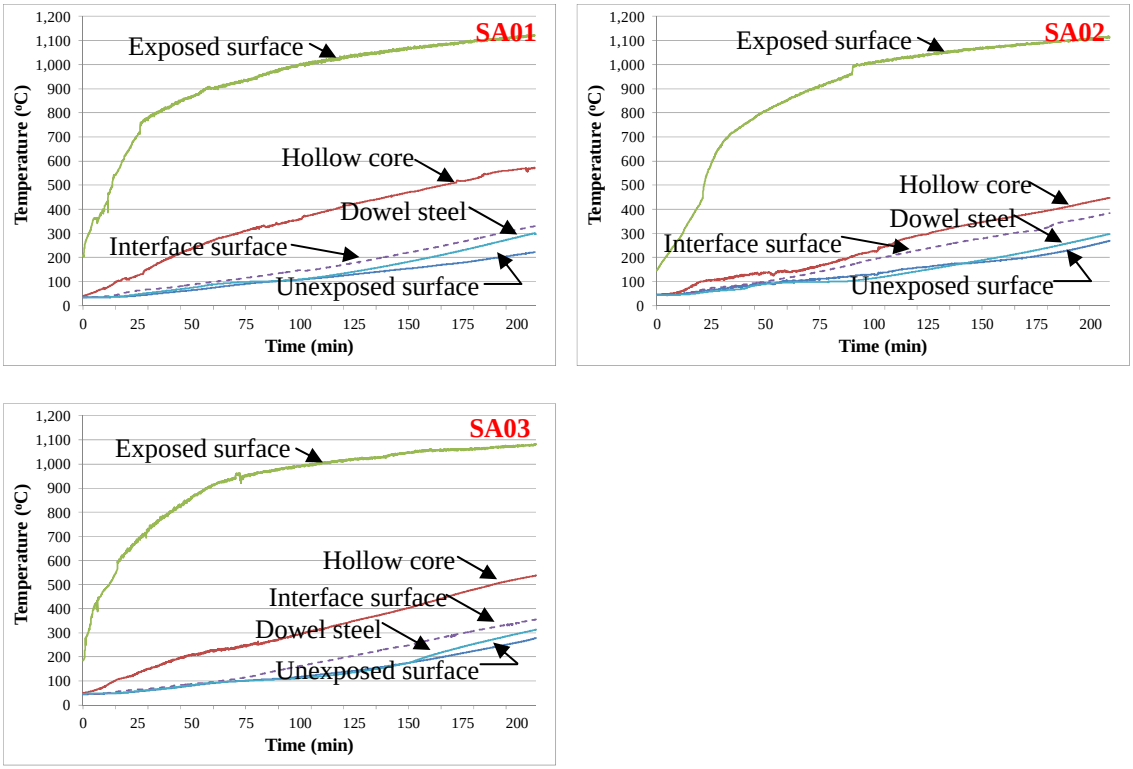

Figure 3.27 Temperature vs. time for SA01 -SA03

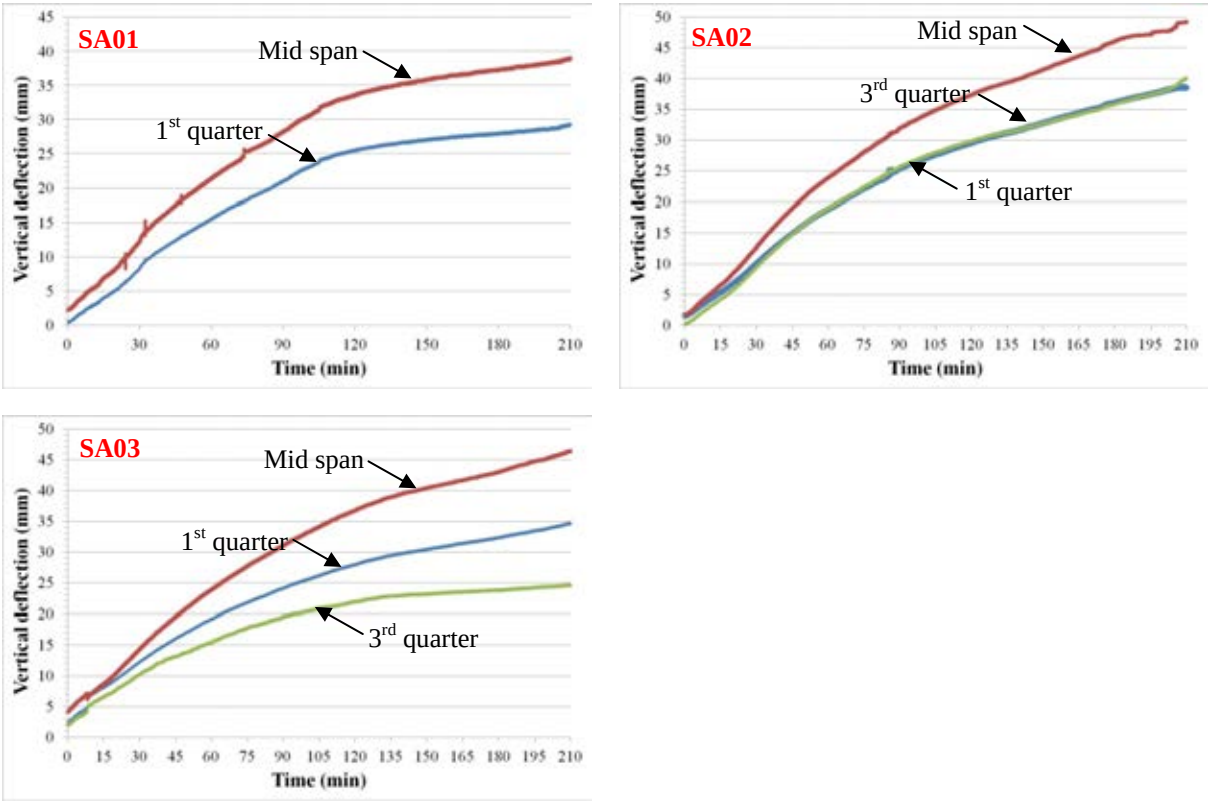

Figure 3.28 Vertical deflection vs. time for SA01 -SA03

3.5.3.1 SA01

SA01 was subjected to the applied load with a load ratio of 0.3. The slab thickness was 100 mm and designated as the exterior span. The average temperature of the unexposed surface at the beginning of the test was 35°C. After the 210-min heating period, the specimen remained intact without collapse. The maximum vertical deflection was 39 mm at mid-span while the average temperature of the exposed surface was 1121°C. The temperature gradients between the exposed surface and unexposed surface, between the exposed surface and the concrete topping-slab interface and between the exposed surface and hollow core were 900°C, 792°C and 551°C, respectively. Although the specimen did not collapse, the mean temperature rise of the unexposed surface exceeded 140°C failing the insulation criterion according to ISO834 [12] after 170-min heating duration. Based on the post-fire investigation, concrete spalling occurred almost over the entire exposed surface with

an average depth of 10 mm. Further, severe concrete spalling was observed at one edge of the test specimen as shown in Fig. 3.29. Despite the severe concrete spalling, no tendon rupture was observed. A horizontal crack was observed near the interface between the supporting concrete block and the hollow core concrete slab. A horizontal crack was also observed at the interior end on the unexposed surface at the interface between concrete topping and supplementary concrete block as shown in Fig. 3.29.

3.5.3.2 SA02

SA02 was also designated as the exterior span as SA01 but was subjected to the load ratio of 0.6. The average temperature of the unexposed surface at the beginning of the test was 44^{o}C. After the 210-min heating duration, the test specimen did not collapse with the maximum vertical deflection of 49.3 mm at mid-span, which was slightly higher compared with SA01. The temperature gradients between the exposed surface and unexposed surface, between the exposed surface and the concrete topping-slab interface and between the exposed surface and hollow core were 845^{o}C, 730^{o}C and 666^{o}C, respectively. The mean temperature rise of the unexposed surface exceeded 140^{o}C after 155-min heating duration. Interestingly, virtually no concrete spalling was observed at the exposed surface of the specimen. However, similar horizontal cracks to SA01 were also observed at both ends as can be shown in Fig 3.30. Note that concrete spalling of the supporting concrete block was an extraneous damage which occurred after the fire test.

3.5.3.3 SA03

SA03 was designated as the interior span with the load ratio of 0.3. Based on the test results, the test specimen remained intact without collapse after the 210-min heating duration. The maximum vertical deflection was 46.4 mm, which was lower compared with SA01 at the same load ratio. The average temperature of the unexposed surface at the beginning of the test was 46^{o}C and the maximum temperature rise exceeded 140^{o}C after 158-min heating duration. The temperature gradients between the exposed surface and unexposed surface, between the exposed surface and the concrete topping-slab interface surface and between the exposed surface and hollow core after the 210-min heating duration were 804^{o}C, 727^{o}C and

545^{o}C, respectively. Neither concrete spalling nor transverse crack was observed on the exposed surface of the specimen. Nevertheless, horizontal cracks were observed at both ends of the specimen as shown in Fig 3.31.

(a)

(b)

(c)

Figure 3.29 SA01 after fire test: (a) bottom surface (b) exterior end and (c) interior end

(a)

(b)

(c)

Figure 3.30 SA02 after fire test: (a) bottom surface (b) exterior end and (c) interior end

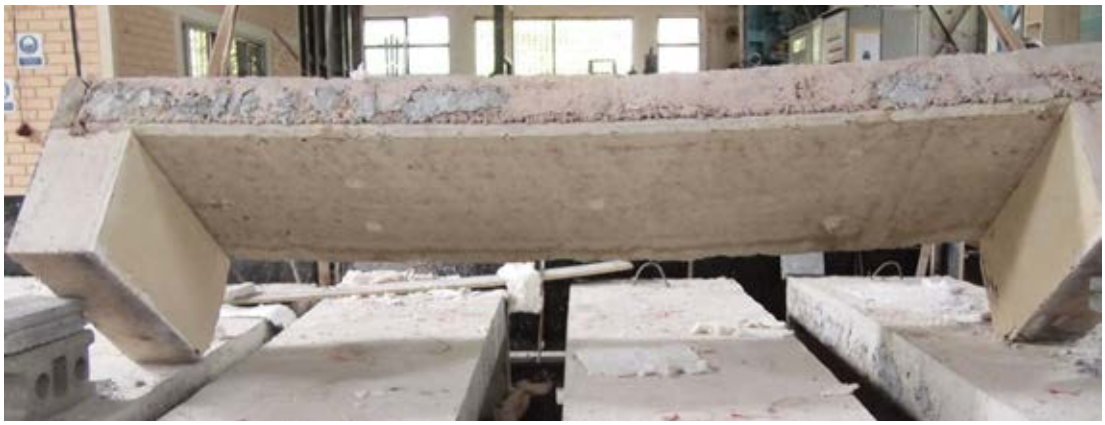

(a)

(b)

(c)

Figure 3.31 SA03 after fire test: (a) bottom surface (b) interior end (top view) and (c) interior end (side view)

3.6 Summary

Based on the results obtained from the fire test, the following conclusions may be drawn on the fire performance of hollow core concrete slabs.

3.6.1 Effect of heating duration

Based on the results of test program 1 for the simply supported specimens with a constant thickness of 120 mm and a fixed load ratio of 0.3, concrete spalling occurred over 0%, 77% and 100% of the exposed surface with the maximum depth of 0 mm, 3 mm and 10 mm, respectively, for TB01, TB02 and TB03. It can thus be concluded that the level of concrete spalling varies proportionally with the heating duration, the longer the heating duration the more severe concrete spalling. However, concrete spalling may not be a crucial factor to the failure of the specimen since the maximum depth of concrete spalling for TB03 is less than the concrete cover at the time of failure. The failure of TB03 is observed to be due to the occurrence of a transverse crack after 82 minutes of standard fire exposure.

3.6.2 Effect of thickness of slab and load ratio

Based on the test results of test program 2, the fire-resistance ratings of simply supported specimens LB01, LB03 and LB05 with the same load ratio of 0.3 but with different thicknesses of 100 mm, 120 mm and 150 mm, respectively, are 107, 91 and 66 minutes while the maximum vertical deflections at mid-span are 140.3, 58.1 and 51.2 mm. It can thus be concluded that even though thicker hollow core concrete slabs lead to smaller vertical deflections, the fire resistance ratings may be lower. This result may be counter-intuitive in that thicker reinforced concrete slabs are generally designated with higher fire-resistance ratings [14]. For LB02, LB04 and LB06 with the same load ratio of 0.6, the fire-resistance ratings are 55, 33 and 39 min, respectively, while the maximum vertical deflections are 91 mm and 38 mm for LB02 and LB04 (40.7 mm for LB07 prior to brittle failure). By comparing between the specimens with the same thickness but with different load ratios, it is seen that the higher load ratio leads to a more rapid collapse. The post-fire investigation also

reveals that the failure of the specimen is mainly due to the occurrence of a transverse crack on the exposed surface. Furthermore, the level of concrete spalling is not significantly affected by the thickness of slab and the load ratio.

3.6.3 Effect of end restraint

Based on the results of test program 3, the specimens SA01, SA02 and SA03 remained intact without collapse after the 210-min heating duration. By comparing to the simply supported specimens with the same thickness of 100 mm and the same load ratios, the specimens with concrete end plugs and concrete topping have significantly better performance in fire. The enhanced fire performance is due to the restraint provided at both ends. In the post-fire investigation of specimens SA01-03, horizontal cracks were observed at both the interior end and the exterior end. During the fire test, the loss of flexural strength caused the specimens to deflect downwards at mid-span and the restraint was induced against rotation at both ends due to the support conditions. For the interior span, the rotational restraint at both ends is confirmed by the appearance of horizontal cracks on the unexposed surface at the interface between concrete topping and the supporting concrete block as can be seen in Fig. 3.29 to Fig. 3.31. The horizontal crack was also observed at the exterior end near the interface between the supporting concrete block and the hollow core concrete slab. The support conditions of SA01-SA03 enhanced the fire resistance performance compared with the simply supported specimens. Fig. 3.32 explains the behavior of a slab with rotational restraint during the fire test. The slab was subjected to the bending moment due to the applied load while the flexural strength drops from M_n to M_{nt} under fire exposure. The slab would collapse when the plastic hinge occurs at three positions. Firstly, the plastic hinge would occur at the support when the flexural strength M_{nt} drops to M_{fire} and the moment at mid-span would increase due to moment redistribution. As the flexural drops further, the slab would collapse once the plastic hinge occurs at mid-span. The failure mechanism of the slab with rotational restraint is shown in Fig. 3.32(c). Based on the test results, the plastic hinge did not occur on SA01-SA03 and the specimens remained intact without collapse during the fire test. The vertical deflections of the specimens were lower compared with the simply

supported specimens with the same level of load ratio. Based on the test results of SA01 and SA02, it is seen that the higher load ratio induces a slightly larger deflection at mid-span. The maximum vertical deflections for SA01 and SA02 are 35 mm and 49.3 mm, respectively. Moreover, SA02 which was designated as the exterior span had higher vertical deflections throughout the fire test compared with SA03 which was designated as the interior span under the same level of load ratio. It can therefore be concluded that the degree of rotational restraint provided by the exterior end is lower compared with the interior end.

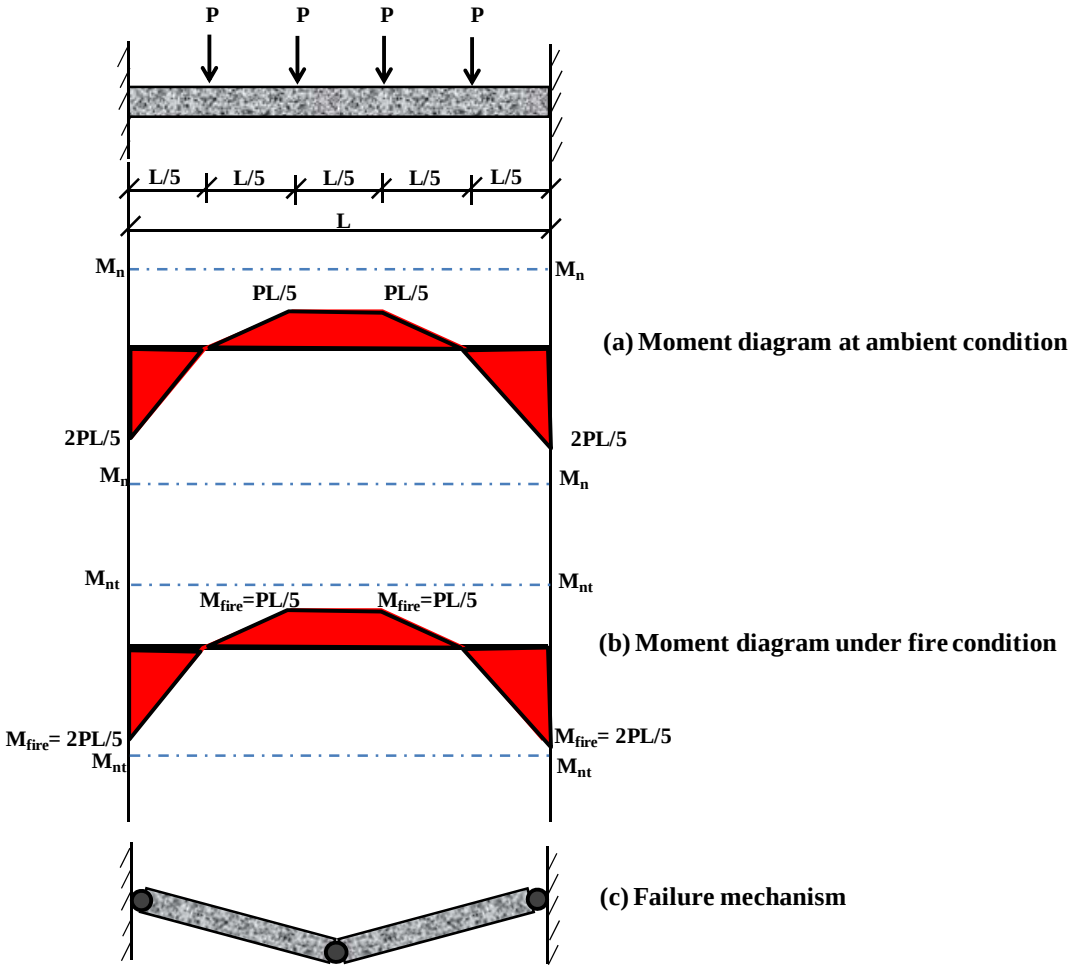

Figure 3.32 Moment diagrams for a slab with rotational restraint under fire

In addition to the rotational restraint, the slab-end beam connection and concrete topping can also provide axial restraint to the specimens at elevated temperatures. When the specimens with end restraint were heated, they would expand and push against the unheated surrounding concrete at the support. The thermal thrust was induced during the fire test due to the axial restraint. The post-fire investigation of specimens SA01-SA03 revealed that the line of thermal thrust was located below the centroidal axis as shown in Fig. 3.29 to Fig.3.31 as observed from the contact surface between the hollow core slab unit and the surrounding structures.

The combined effect of rotational restraint and axial restraint can be illustrated in Fig. 3.33. When the slab is heated, the vertical deflection and the thermal expansion occur while the additional moment due to axial restraint, M_{Δ}, is induced as shown in Fig. 3.33(b). Despite the moment due to axial restraint, the additional moment, M_{th}, is induced along the length of slab because of the rotational restraint at both ends as shown in Fig. 3.33(c). The combined bending moment during the fire test, M_{fire}, is shown in Fig. 3.33(d). The slab will collapse if the flexural capacity is exceeded at three plastic hinge locations. This combined effect can significantly enhance the fire-resistance performance of the slab.

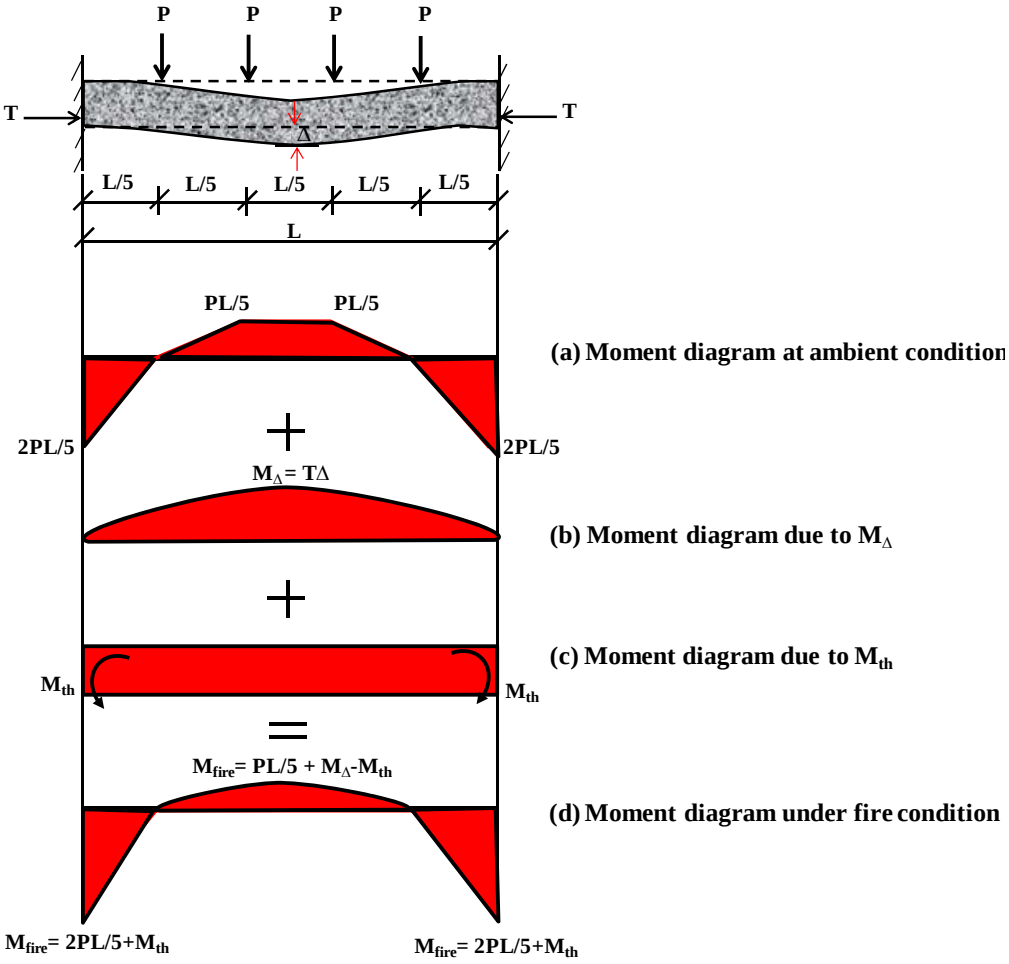

Figure 3.33 Moment diagrams for a slab with rotational restraint and axial restraint under fire

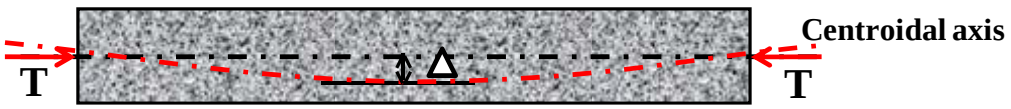

(a) $M_\Delta = T\Delta$

(b) $M_{th} = TZ_o$

Figure 3.34 Free body diagram of a slab with M_Δ and M_{th}

CHAPTER IV

CONCLUSION

The current study aims to investigate the effect of end restraint on the fire resistance performance of typically installed hollow core concrete slabs with slab-end beam connection and concrete topping through a series of fire tests. In order to examine the behavior of the hollow core concrete slabs at elevated temperatures and the effect of end restraint due to slab-end beam connection and concrete topping on the fire performance of hollow core concrete slabs, a series of fire tests were conducted for thirteen hollow core concrete slab specimens using ISO 834 standard fire curve [12]. Ten simply supported specimens without end restraint were tested to examine the effect of heating duration, slab thickness and load ratio. Three specimens were installed with slab-end beam connection and concrete topping with varying end details for the interior span and exterior span.

The test program was divided into three parts. The first part investigates the effect of heat exposure time on the fire-resistance performance of the hollow core concrete slabs. The second part investigates the effect of load ratio and thickness of slab on the fire-resistance performance of the hollow core concrete slabs. For the first and second test programs the effect of end restraint is not considered. The third test program investigates the effect of the end restraint on the fire-resistance performance of hollow core concrete slabs.

Based on the test results, it can be concluded that the level of concrete spalling varies proportionally with the heating duration, the longer the heating duration the more severe concrete spalling. However, concrete spalling may not be a crucial factor to the failure of the specimen.

It can be concluded from the test results of the specimens with the same level of load ratio but with different thicknesses, that even though thicker hollow core concrete slabs lead to smaller vertical deflections, the fire resistance ratings may be lower.

The comparison between the specimens with the same thickness but with different load ratios, shows that the higher load ratio leads to a more rapid collapse. The post-fire investigation also reveals that the failure of the specimen is mainly due to the occurrence of a transverse crack on the exposed surface. Furthermore, the level of concrete spalling is not significantly affected by the thickness of slab and the load ratio.

Compared with the simply supported specimens with the same thickness and the same load ratios, the specimens with concrete end plugs and concrete topping have significantly better performance in fire. The enhanced fire performance is due to the restraint provided at both ends. In the post-fire investigation of specimens with concrete end plugs and concrete topping, horizontal cracks were observed at both the interior end and the exterior end. During the fire test, the loss of flexural strength caused the specimens to deflect downwards at mid-span and the restraint was induced against rotation at both ends due to the support conditions. For the interior span, the rotational restraint at both ends is confirmed by the appearance of horizontal cracks on the unexposed surface at the interface between concrete topping and the supporting concrete block. The horizontal crack was also observed at the exterior end near the interface between the supporting concrete block and the hollow core concrete slab.

In addition to the rotational restraint, the slab-end beam connection and concrete topping can also provide axial restraint to the specimens at elevated temperatures. When the specimens with end restraint were heated, they expanded and pushed against the unheated surrounding concrete at the support. The thermal thrust was induced during the fire test due to the axial restraint. The post-fire investigation revealed that the line of thermal thrust was located below the centroidal axis as observed from the contact surface between the hollow core slab unit and the surrounding structures.

The combined effect of rotational restraint and axial restraint can significantly enhance the fire resistance performance of the slabs. When the slab is heated, the vertical deflection and the thermal expansion occur while the additional moment due to axial restraint is induced. Despite the moment due to axial restraint, a counter-balance moment is induced along the length of slab because of the rotational restraint at both ends. The slab will collapse if the flexural capacity is exceeded at three plastic hinge locations. Based on the test results, the plastic hinge did not occur and the specimens remained intact without collapse during the fire test.

Further experimental studies should be conducted to verify the efficacy of the slab-end beam connection and concrete topping in enhancing the fire-resistance performance of the hollow core concrete slab system with different configurations, e.g. span-depth ratio.

REFERENCES

[1] Zheng, W.Z., Hou, X.M., Shi, D.S., and Xu, M.X. Experimental study on concrete spalling in prestressed slabs subjected to fire. Fire Safety Journal 45 (2010) : 283-297.

[2] Bailey, C.G., and Ellobody, E. Fire tests on bonded post-tensioned concrete slabs. Engineering Structures 31 (2009) : 686-696.

[3] Ellobody, E., and Bailey, C.G. Modelling of unbounded post-tensioned concrete slabs under fire conditions. Fire Safety Journal 44 (2009) : 159-167.

[4] Gales, J., Bisby, L.A., and Gillie, M. Unbonded post tensioned concrete in fire: A review of data from furnace tests and real fires. Fire Safety Journal 46 (2011) : 151-163.

[5] Lim, L., Buchanan, A.H., and Moss, P. J. Restraint of fire-exposed concrete floor systems. Fire and Materials 28 (2004) : 95-125.

[6] Chang, J., Buchanan, A.H., Dhakal, R.P., and Moss, P.J. Hollow-core concrete slabs exposed to fire. Fire and Materials 32 (2008) : 321-331.

[7] Fellinger, J., Stark, J., and Walraven, J. Shear and anchorage behavior of fire exposed hollow core slabs. Heron 50 4 (2005) : 279-301.

[8] Huang, Z.H. The behaviour of reinforced concrete slabs in fire. Fire Safety Journal 45 (2010) : 271-282.

[9] Bailey, C.G., and Ellobody, E. Whole-building behaviour of bonded post-tensioned concrete floor plates exposed to fire. Engineering Structures 31 (2009) : 1800-1810.

[10] FeBe. Résistance au Cisaillement de Dalles Alveolées Précontraintes, Laboratorium voor Aanwending der Brandstoffen en Warmteoverdracht. Belgium, Studiecommissie SSTC (1998)

[11]American Concrete Institute (ACI). Code requirements for determining fire resistance of concrete and masonry construction assemblies, ACI 216.1-07/TMS-216-07 : 2007.

[12]International Organization for Standardization (ISO). Fire-resistance tests : element of building constructions-Part 1:General requirements, ISO834-1,Switzerland : 1999.

[13]Buchanan, A.H. Structural design for fire safety. by John Wiley & Sons. Chichester : 2001.

[14]Ali, F., Nadjai, A., and Abu-Tair, A. Explosive spalling of normal strength concrete slabs subjected to severe fire. Material and Structures (2010).

[15]Cooke, G.M.E. Behaviour of precast concrete floor slabs exposed to standardised fires. Fire Safety Journal 36 (2001) : 459-475.

[16]Concrete Reinforcing Steel Institute (CRSI). Reinforced concrete fire safety. Illinois: 1980.

[17]Girhammer, U.A., and Pajari, M. Test and Analysis on shear strength of composite slabs of hollow core units and concrete topping. Construction and Building Materials 22 (2008) : 1708-1722.

[19]American Society for Testing and Materials (ASTM). Standard Test Methods for Fire Tests of Building Construction and Materials, ASTM E119-12a : 2012.

[20]American Concrete Institute (ACI), Building Code Requirements for Structural Concrete, ACI 318-11 : 2011.

[21]European Committee for Standardisation (CEN). Eurocode 2: Design of concrete structures, Part1.2: General Rules-Structural Fire Design, EN 1992-1-2, London: British Standards Institution : 2004.

[22]American Society of Civil Engineers (ASCE), Minimum Design Loads for Building and Other Structures, ASCE 7-10 : 2010.

APPENDIX

Load Ratio Calculation

This section presents the calculation of the flexural capacity of the hollow core concrete slab at normal temperature and the load ratio for the experimental investigation.

A.1 Stress in prestressing steel at nominal flexural strength

The stress in prestressing steel at nominal flexural strength (f_{ps}) can be calculated according to ACI 318-11 [20] as follows:

$$f_{ps} = f_{pu}\left\{1 - \frac{\gamma_p}{\beta_1}\left[\rho_p \frac{f_{pu}}{f_c'} + \frac{d}{d_p}(\omega - \omega')\right]\right. \quad \text{(A-1)}$$

where f_{ps} = stress in prestressing steel at nominal flexural strength (MPa)

f_{pu} = specified tensile strength of prestressing steel (MPa)

f_c' = specified compressive strength of concrete (MPa)

β_1 = factor relating depth of equivalent rectangular compressive stress block to neutral axis depth

= $0.85 - \frac{0.05}{7}(f_c' - 28)$

γ_p = factor for type of prestressing steel = 0.28

ρ_p = ratio of area of prestressing steel in flexural tension zone = A_{ps}/bd_p

ω = tension reinforcement index = 0

ω' = compression reinforcement index = 0

d = distance from extreme compression fiber to centroid of longitudinal tension reinforcement (mm)

d_p = distance from extreme compression fiber to centroid of prestressing steel (mm)

A_{ps} = area of prestressing steel in flexural tension zone (mm^2)

b = width of specimen (mm)

A.2 Flexural capacity

The flexural capacity of the hollow core concrete slab at normal temperature can be computed by balancing the tension force in the prestressing steel and the compression force due to the equivalent rectangular stress block in concrete with the depth calculated based on the equation below [21].

$$a = \frac{A_{ps} \times f_{ps}}{\beta_1 \times f'_c \times b} \quad \text{(A-2)}$$

For the slab with concrete topping, the transformed section can be used.

$$b_{tr} = b \frac{E_c}{E_t} \quad \text{(A-3)}$$

where E_c = Modulus of elasticity for hollow core concrete slab (MPa)

E_t = Modulus of elasticity for concrete topping (MPa)

b_{tr} = Width of transformed specimen (mm)

The depth of the equivalent rectangular stress block for the slab with concrete topping are calculated as follows.

$$a = \frac{A_{ps} \times f_{ps}}{\beta_1 \times f'_t \times b_{tr}} \quad \text{(A-4)}$$

where f'_t = specified compressive strength of concrete topping (MPa)

The flexural capacity can be computed using the following expression.

$$\phi M_n = \phi A_{ps} f_{ps} \left(d_p - \frac{a}{2}\right) \quad \text{(A-5)}$$

where M_n = nominal flexural strength (N-mm)

a = depth of equivalent rectangular stress block (mm)

ϕ = 0.9

A.3 Load ratio

The load ratio can be computed as the ratio between the applied bending moment due to the specified live load plus the existing dead load and the flexural capacity of the slab. For the current study, two applied load combinations are assumed.

- Load combination 1: w_{fi} = 1.2*DL*+0.5*LL*, as proposed by ASCE7-10 [22], to simulate a 50% reduction of live load during the fire. This load combination has been used for all of the specimens in test program 1 as well as LB01, LB03 and LB05 in test program 2 and SA01 in test program 3.

- Load combination 2: w_{fi} = 1.0*DL*+1.0*LL*, to simulate typical service loads and is more severe compared with load combination 1. LB02, LB04 and LB06 in test program 2 and SA02 and SA03 in test program 3 are designated with this load combination.

in which w_{fi} = factored load per unit length of slab in case of fire (N/m)

DL = dead load (N/m^2)

LL = design live load (N/m^2)

Because the external loads are applied using the mechanical device as shown in Fig. 3.4, the bending moment can be calculated as

$$M_{fi} = \frac{3w_{fi}L^2}{20} \quad \text{(A-6)}$$

where L = span length (m)

From which the load ratio can be calculated by the following expression.

$$\text{Load ratio} = \frac{M_{fi}}{\phi M_n} \quad \text{(A-7)}$$

A.4 Calculation results

The flexural capacity and the load ratio computed based on the above procedures for all of the specimens can be summarized in Table A.1 and Table A.2, respectively.

Table A.1 Summary of the flexural capacity calculation

Specimen	f_{pu} (MPa)	f_c' (MPa)	f_t' (MPa)	β_1	d_p (mm)	A_{ps} (mm^2)	ρ_p	f_{ps} (MPa)	a (mm)	Flexural capacity : ϕM_n (N-m)
TB01	1850	35	-	0.8	97.5	75.42	0.0013	1,805.9	8.1	11,454.6
TB02	1850	35	-	0.8	97.5	75.42	0.0013	1,805.9	8.1	11,454.6
TB03	1850	35	-	0.8	97.5	75.42	0.0013	1,805.9	8.1	11,454.6
TB04	1850	35	-	0.8	97.5	75.42	0.0013	1,805.9	8.1	11,454.6
LB01	1850	35	-	0.8	77.5	75.42	0.0016	1,794.5	8.1	8,949.4
LB02	1850	35	-	0.8	77.5	75.42	0.0016	1,794.5	8.1	8,949.4
LB03	1850	35	-	0.8	97.5	75.42	0.0013	1,805.9	8.1	11,454.6
LB04	1850	35	-	0.8	97.5	75.42	0.0013	1,805.9	8.1	11,454.6
LB05	1850	35	-	0.8	127.5	75.42	0.0010	1,816.3	8.2	15,216.1
LB06	1850	35	-	0.8	127.5	75.42	0.0010	1,816.3	8.2	15,216.1
SA01	1850	35	24	0.8	127.5	75.42	0.0010	1,816.3	14.4	14,833.5
SA02	1850	35	24	0.8	127.5	75.42	0.0010	1,816.3	14.4	14,833.5
SA03	1850	35	24	0.8	127.5	75.42	0.0010	1,816.3	14.4	14,833.5

Table A.2 Summary of the load ratio calculation

Specimen	DL (N/m)	LL (N/m)	w_{fi} (N/m)	M_{fi} (N-m)	ϕM_n (N-m)	Load ratio	
TB01	1,124.3	8,730	5,714.3	3,780.0	11,454.6	0.33	(use 0.30)
TB02	1,124.3	8,730	5,714.3	3,780.0	11,454.6	0.33	(use 0.30)
TB03	1,124.3	8,730	5,714.3	3,780.0	11,454.6	0.33	(use 0.30)
TB04	1,124.3	8,730	5,714.3	3,780.0	11,454.6	0.33	(use 0.30)
LB01	1,034.9	6,716	4,599.9	3,042.8	8,949.4	0.34	(use 0.30)
LB02	1,034.9	6,716	7,751.0	5,127.3	8,949.4	0.57	(use 0.60)
LB03	1,124.3	9,077	5,887.4	3,894.5	11,454.6	0.34	(use 0.30)
LB04	1,124.3	9,077	10,200.9	6,747.9	11,454.6	0.59	(use 0.60)
LB05	1,300.7	11,600	7,360.7	4,869.1	15,216.1	0.32	(use 0.30)
LB06	1,300.7	11,600	12,900.6	8,533.7	15,216.1	0.56	(use 0.60)
SA01	1,740.8	10,950	7,564.0	5,003.6	14,833.5	0.34	(use 0.30)
SA02	1,740.8	10,950	12,690.8	8,395.0	14,833.5	0.57	(use 0.60)
SA03	1,740.8	10,950	7,564.0	5,003.6	14,833.5	0.34	(use 0.30)

BIOGRAPHY

Mr. Chaiyatorn Kositsornwanee was born in Bangkok, Thailand in 1986. He received his Bachelor's degree in Civil Engineering from Chulalongkorn University in 2009. After working in an engineering consultant firm for 2 years, he decided to continue his graduate study in the field of structural engineering at the Department of Civil Engineering, Chulalongkorn University in 2011. During his Master's study, he was granted a scholarship by JASSO to participate in the Young Scientist Exchange Program (YSEP) at Tokyo Institute of Technology for 6 months in 2012.